UMTRI-88-19

STEERING SYSTEM ABDOMINAL IMPACT TRAUMA

Guy S. Nusholtz
Patricia S. Kaiker
R. Jeff Lehman

Final Report to:

Motor Vehicle Manufacturers Association
320 New Center Building
Detroit, Michigan 48202

April 30, 1988

UMTRI The University of Michigan
Transportation Research Institute

STEERING SYSTEM ABDOMINAL IMPACT TRAUMA

Guy S. Nusholtz, Patricia S. Kaiker, and R. Jeff Lehman

MVMA Project No. 7131 Final Report

Project Director: Guy S. Nusholtz

Technical Report Documentation Page

1. Report No.	2. Government Accession No.	3. Recipient's Catalog No.
UMTRI-88-19		

4. Title and Subtitle	5. Report Date
STEERING SYSTEM ABDOMINAL IMPACT TRAUMA	April 1988
	6. Performing Organization Code
	8. Performing Organization Report No. UMTRI-88-19
7. Author(s) G.S. Nusholtz, P.S. Kaiker, and R.J. Lehman	
9. Performing Organization Name and Address University of Michigan Transportation Research Institute 2901 Baxter Road Ann Arbor, Michigan 48109-2150	10. Work Unit No. (TRAIS) 362683 11. Contract or Grant No. 7131
12. Sponsoring Agency Name and Address Motor Vehicle Manufacturers Association 320 New Center Building Detroit, Michigan 48202	13. Type of Report and Period Covered FINAL REPORT 8/1/86 - 8/31/87 14. Sponsoring Agency Code

15. Supplementary Notes

16. Abstract A series of impact tests to the abdomen and thorax of unembalmed cadavers was conducted using a rigid, curved steel bar to simulate the lower portion of the steering wheel rim. The test matrix used involved impacts to different regions of the thorax and abdomen at different impact velocities and with several low-velocity impacts on each subject prior to conducting high-velocity impact. These test conditions were originally established to investigate the effects of various test conditions (e.g., pressurization versus no pressurization) and variability in test results among subjects under similar conditions.

Subsequent to data collection, the goals of the project were changed to focus on evaluation of different proposed injury criteria. Analysis routines were developed to calculate values for the different injury criteria but, because of the multiple impacts on each subject and differences in impact locations between tests, and because of the high correlations among the different injury criteria for the test conditions, evaluation and comparison of the proposed injury criteria could not be meaningfully made.

The test results point out the importance of the location of the impact to liver injury, and provide new data on force-deflection characteristics for the mode of impact used in these tests.

17. Key Words	18. Distribution Statement
Impact response Thorax Abdomen Injury Steering wheel	Unlimited

19. Security Classif. (of this report)	20. Security Classif. (of this page)	21. No. of Pages	22. Price
None	None	72	

Reproduction of completed page authorized

ACKNOWLEDGEMENTS

The authors wish to acknowledge the assistance of Donald F. Huelke, Steven C. Richter, and Colleen Jones.

TABLE OF CONTENTS

Page

LIST OF TABLES

LIST OF FIGURES

I. INTRODUCTION

1.0 Organization of Report

MVMA Project No. 7131 was a continuation of Project Nos. 6131 and 5131 concerning abdominal trauma caused by impact with a steering wheel assembly. This final report for fiscal year 1987 documents the experimental procedures used to conduct the thoraco-abdominal impact tests and the analytical procedures used to obtain the dynamic response variables associated with five thoracic injury criteria which the MVMA Biomechanics Subcommittee is currently proposing as possible predictors of abdominal trauma. The report contains:

- a description of all the impact tests from 1985-1986,
- summaries of the dynamic variables and injuries,
- a discussion of the impact and injury response of the human cadaver for these test conditions.

2.0 Background and Objectives

Testing Objectives - During 1984-1985, previous biomechanics research conducted at UMTRI was reviewed and evaluated as part of the task of designing a protocol for simulations of steering wheel assembly impacts which use the unembalmed human cadaver as a surrogate for the live human. As a result of the review, it was decided to investigate abdominal impact response in terms of: (1) the effect of pulmonary repressurization, (2) the repeatability of results from cadaver surrogates, (3) the effect of impact contact region on the injuries produced, and (4) providing information for comparison of the impact response of the repressurized cadaver surrogate to that of the porcine surrogate experiments of Lau, Horsch, Viano, and Andrzejak [1].[1]

---

[1] Number in bracket identifies references located at the end of the report.

The test protocol developed in fiscal year 1985[2] was followed for multiple thoraco-abdominal testing of one unembalmed human cadaver during Project 6131. Analysis of the data indicated that this type of blunt impact testing could be useful in characterizing the impact response of the abdominal region, but the results obtained from one subject were not sufficient to draw conclusions about the effects of the experimental parameters on abdominal trauma. Therefore, it was decided to continue the multiple thoraco-abdominal impact simulations in Project 7131. In addition, as suggested by the MVMA Biomechanics Subcommittee, the test protocol was modified to include procedures for repressurizing the abdominal vascular system in order to investigate abdominal impact response also in terms of the effect of vascular repressurization of the abdominal cavity. In order to accomplish the project goals, a protocol was developed that would subject each cadaver to multiple impacts at low velocities and to a single impact at a high velocity. It was believed that the multiple low-velocity impacts would not damage the subject and that the impact response of the high-velocity impact could be related to injury and assist in the evaluation of tolerance levels. This assumption was found to be false. To understand how the test protocol attempted to accomplish the project goals, it is instructive to look at the test design.

Test Design - Given that a test ***series*** consists of one or multiple impacts having the same initial conditions, the test design included seven series (A-G) of low-velocity thoraco-abdominal impacts to seven unembalmed human cadavers, plus two series of a single high-velocity abdominal impact to five unembalmed human cadavers. Eighty-three impacts were

---

[2]The testing protocols used in this research program were approved by The University of Michigan Medical Center and followed guidelines established by the U.S. Public Health Service and those recommended by the National Academy of Sciences, National Research Council.

conducted at low velocities (1.3-3.9 m/s) and five impacts were conducted at high velocities (6.5-10.8 m/s). The test matrix is summarized in Table 1.

The effect of pulmonary and vascular repressurization was to be investigated by contrasting test series having the same initial conditions except for the presence or absence of repressurization of vascular/pulmonary systems. For example, Series A was to be contrasted to Series F and G as well as to Series H and I tests.

The repeatability of results from cadaver surrogates was to be investigated by contrasting individual tests within a series, and by contrasting similar series among subjects. For example, Series A tests on the same subject were to be contrasted to each other as well as to the Series A tests on different subjects.

The effect of impact contact region was to be investigated by contrasting test series having the same initial conditions except for impact contact region. For example, Series B was to be contrasted to Series A and Series C.

The tests also were designed to collect variables similar to those collected in the porcine surrogate experiments of Lau, Horsch, Viano, and Andrzejak [1], e.g., steering rim force, impact velocity, pendulum acceleration, spinal acceleration, and pulmonary/abdominal vascular pressure.

Calculation of Injury Criteria Values - During meetings with the MVMA Biomechanics Subcommittee, subsequent to completion of the impact testing, it was decided that rather than studying the effects of the experimental parameters established in the original objectives and used in developing the test matrix, an analysis should be directed toward assisting in the evaluation of five ***thoracic*** injury criteria as predictors for ***abdominal*** trauma--the Deflection Criterion, the Viscous Criterion, the $V_{max}C_{max}$ Criterion, the Specific Absorbed Energy Criterion, and the Spinal Acceleration Criterion--in terms of calculating their numerical values from the experimental data and information. Therefore, the focus of the analysis presented in this report was to develop the tools needed to

TABLE 1

Test Design

Number of "Non-injurious" Low-Velocity Tests	Series	Contact Region	Repressurization
26	A	Abdominal	none
3	B	Rib 10	none
14	C	Below Sternum	none
11	D	Below Sternum	pulmonary
12	E	Below Sternum	pulmonary/cardiovascular
4	F	Abdominal	cardiovascular
13	G	Abdominal	pulmonary/cardiovascular
Subtotal Tests = 83	Series = 7		

Number of "Non injurious" Low-Velocity Tests	Series	Contact Region	Repressurization
1	H	Abdominal	none
4	I	Abdominal	pulmonary/cardiovascular
Subtotal Tests = 5	Series = 2		

determine the parameters for computation of values for each of the five injury criteria from the dynamic test data and descriptive information. Because of limited funds, only the high-velocity tests plus one low-velocity test were used to compute values for the five injury criteria.

Although it is not possible to relate the injury criteria values to the observed injuries directly because of (1) the multiple impact testing, (2) the different contact regions, and (3) the different velocities used in these experiments, it is possible to evaluate the five criteria in terms of the amount of energy transferred to, or absorbed by, a test subject [1, 10, 13]. In addition, a perplexing problem concerns ambiguities that arise when injuries are described as "thoracic," or "abdominal," or are lumped together for one "body region" score, as opposed to not being lumped together, as in scoring for each "organ."

II. METHODOLOGY

1.0 Experimental Techniques

The techniques used to perform the impact tests are outlined below. Further detail on these procedures can be found in the references [2, 3, 6-9].

1.1 Pneumatic Ballistic Pendulum Impact Device

The impact device (Figure 1) consists of a 25 kg ballistic pendulum mechanically coupled to the UMTRI cannon which was used as the energy source. The cannon is an air reservoir with a ground and honed cylinder carefully fitted with a metal-alloy piston. The piston is connected to the ballistic pendulum with a nylon cable. Compressed air from the air reservoir chamber propels the piston through the cylinder, accelerating the ballistic pendulum to become a free-traveling impact. A magnetic digital displacement transducer is rigidly affixed to the side of the pendulum.

GMRL Steering Wheel Model - The pendulum striker is a physical model of the lower rim of a steering wheel, as shown in Figure 2 [1, 5, 6]. This physical model was described by John Horsch at the 29th Stapp Car Crash Conference [5]. The striker can be simply described as the rigid lower rim of a steering wheel attached to a rigid column support. It is not directly related to any production steering wheel assembly. Rigidly mounted at the base of the column support for the replica of the steering wheel is an inertia-compensated load cell. A triaxial accelerometer is rigidly affixed to the column support for the "steering wheel rim," as shown in the Figure 2 (inset.)

1.2 Subject Preparation and Instrumentation

The unembalmed cadavers used in these tests were obtained from The University of Michigan Department of Anatomy and stored in a cooler at 4 degrees centigrade. All cadavers were x-rayed as part of the screening for anomalies, surgical implants, and pre-existing injuries.

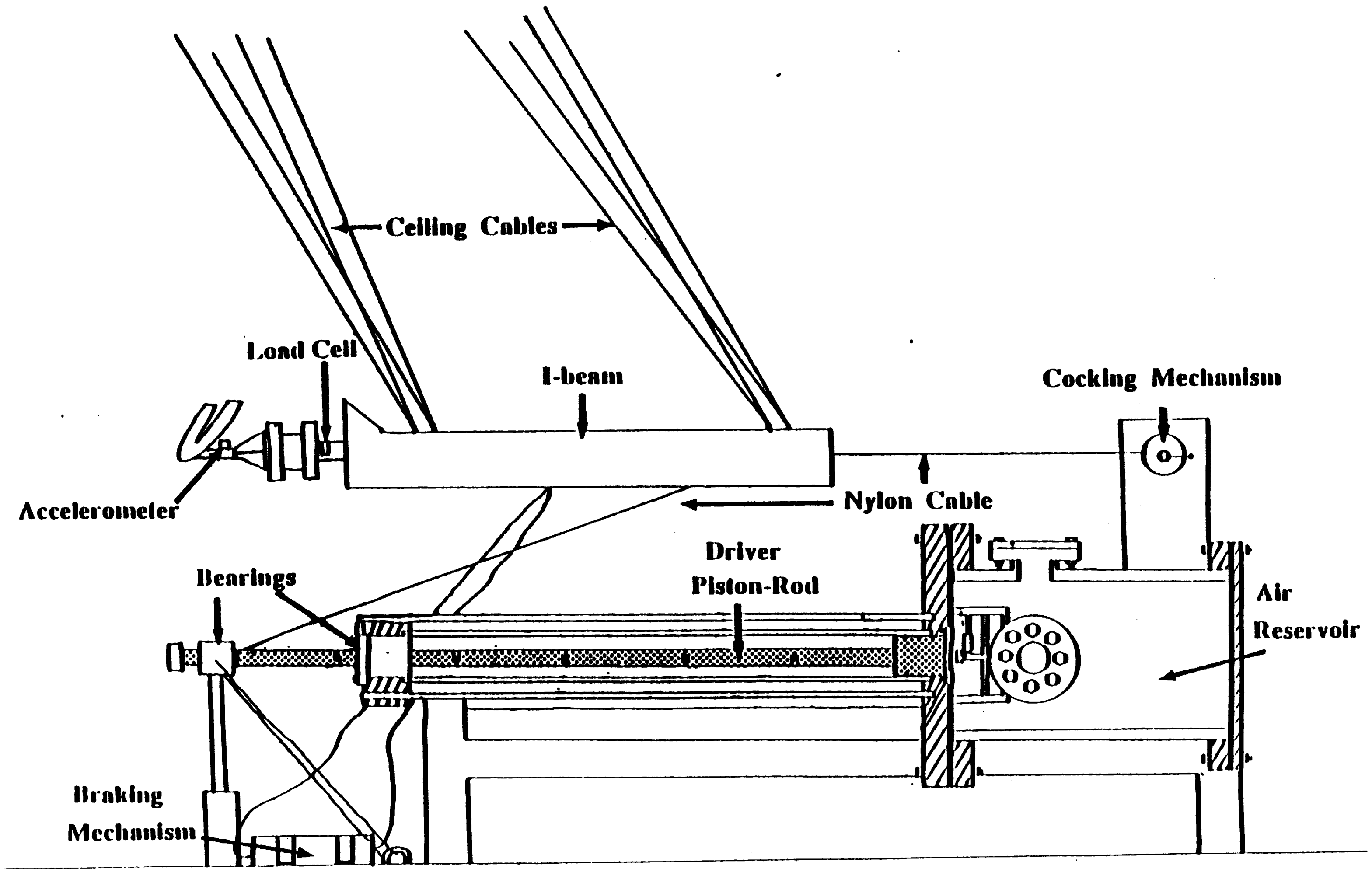

Figure 1. UMTRI Pneumatic Ballistic Pendulum

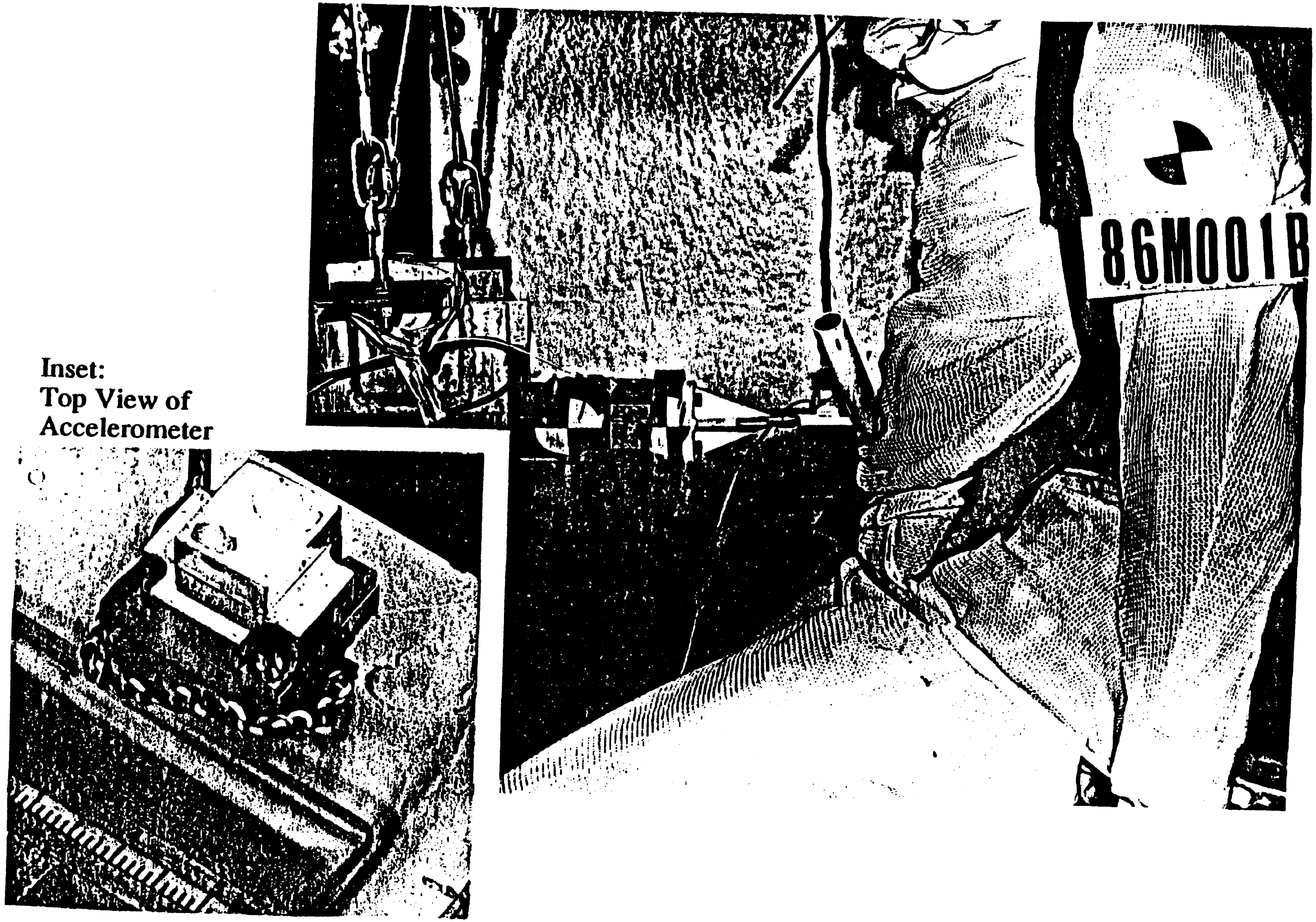

Figure 2. GMRL Steering Wheel Model

Cadavers accepted for testing were measured using standard anthropometric techniques. Next, the cadavers were sanitarily and surgically prepared, dressed in vinyl and cotton clothing, and fitted with head and torso harnesses.

Surgical instrumentation of the subjects included rigidly affixing a triaxial accelerometer mounting platform on thoracic vertebra T12, inserting a tube for pulmonary repressurization, inserting a tube and catheters for abdominal vascular repressurization, and the final sealing of incisions after the transducers had been attached to the mounting platform or tubes.

T12 Triaxial Accelerometer Mounting Platform - To surgically implement a cadaver with a rigid attachment for the triaxial accelerometer cluster, a deep incision is made over the T12 thoracic vertebra and supports for the accelerometer mount are anchored bilaterally on the lamina. The mount is also secured by a screw inserted into the vertebral process, and acrylic is applied under and around the mount to ensure rigidity (Figure 3).

Pulmonary Tracheal Tube - A tracheotomy is performed to place and secure a tube in the trachea. Figure 4 shows the tracheal tube and pressure relief valve.

Cardiovascular Tube and Catheters - Surgical insertion of Foley catheters follows three patterns, depending on whether access through the femoral arteries is possible (Figure 5). Through an incision in the femoral artery, a catheter is guided up the arterial system, where the balloon occludes the aortic termination. Another catheter is guided through an incision in the common carotid artery into the descending aorta to occlude it slightly above the diaphragm. When the femoral arteries cannot be used due to plaque accumulation, either a double balloon catheter is used to occlude the aorta below the diaphragm and at the common iliac arteries, or two catheters, one in each common carotid artery, are used to occlude the aorta below the diaphragm and at the common iliac arteries. In addition, through an incision in the carotid artery, a cardiovascular tube is inserted and secured. All incisions are sealed to contain body fluids.

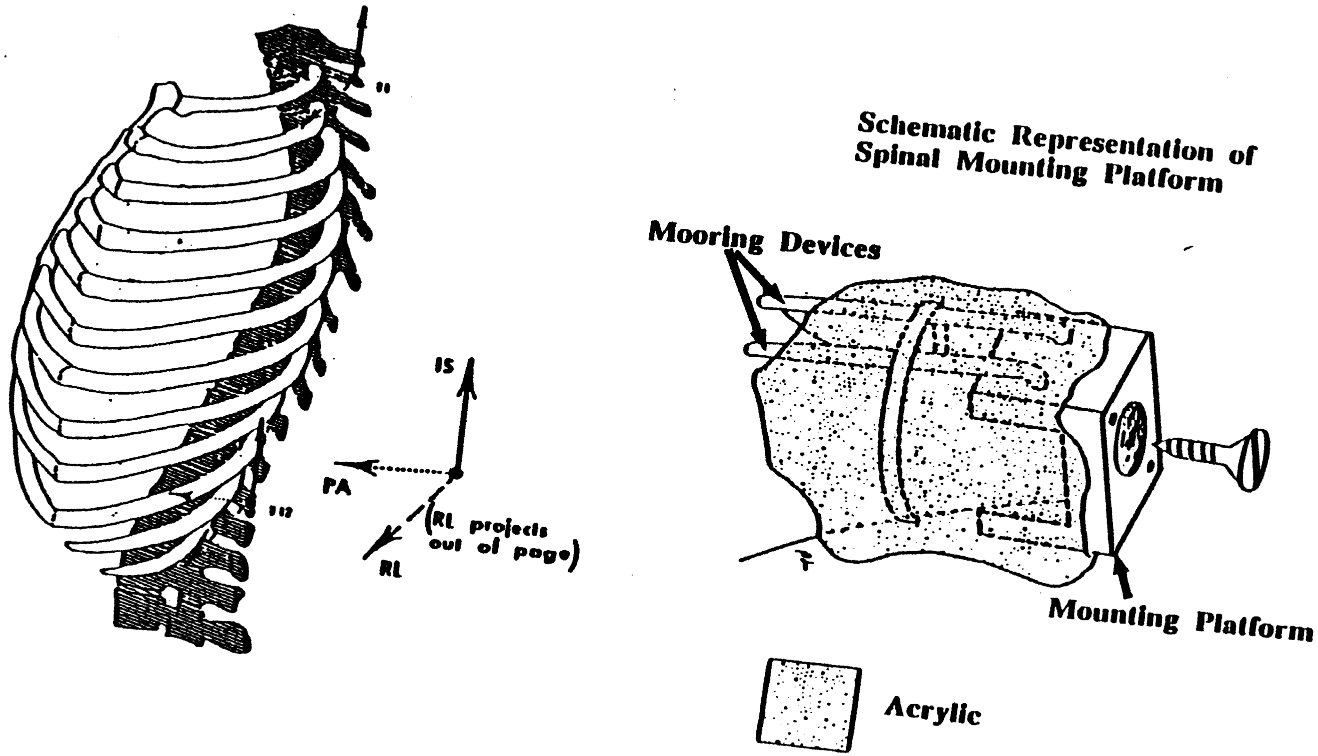

Figure 3. T12 Triax

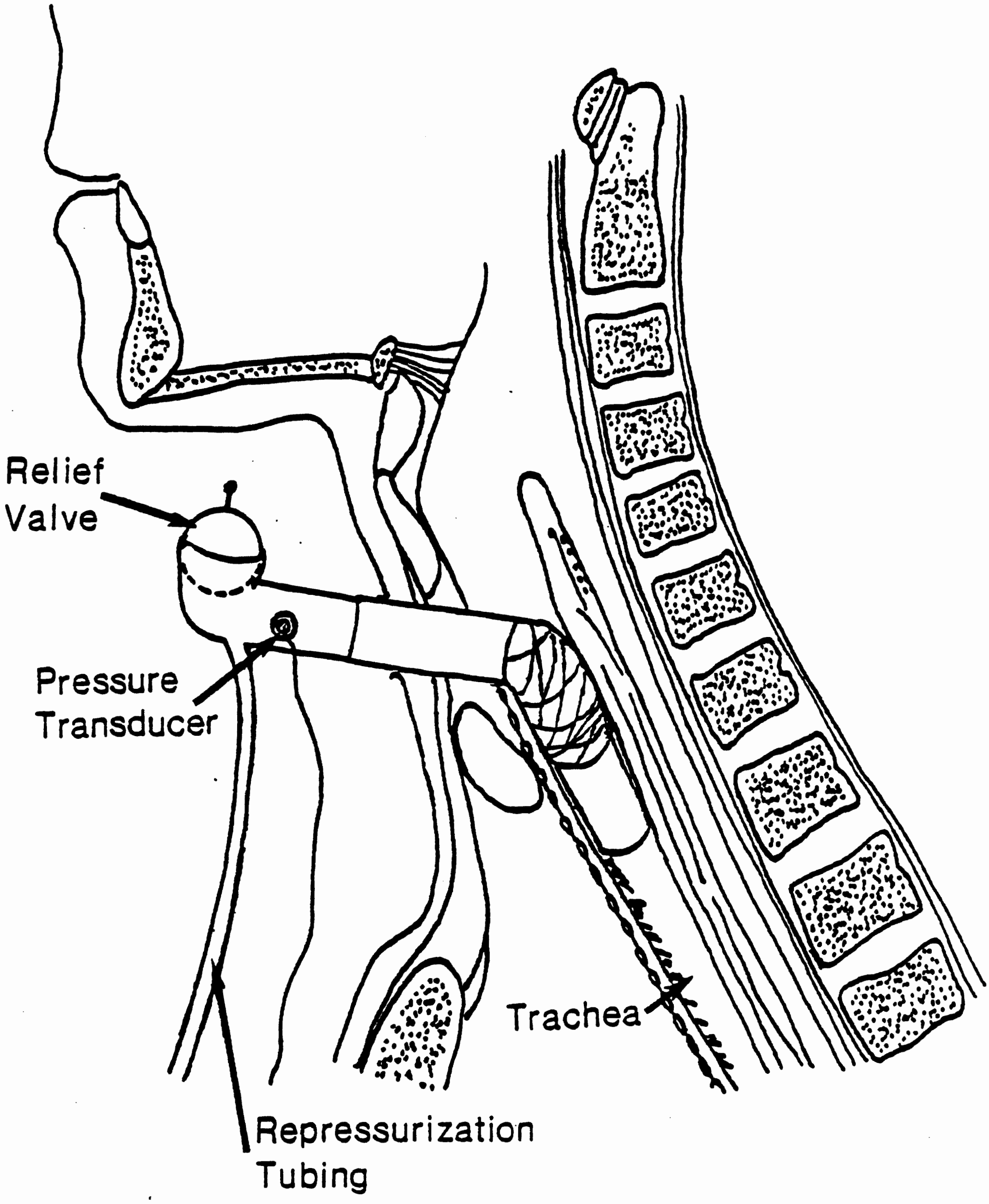

Figure 4. Pulmonary Repressurization

Mechanical instrumentation of the subjects included screwing a triaxial accelerometer in its mounting casing onto the thoracic vertebra T12 mounting platform, attaching a steel digital displacement transducer cable to the sealed incision at T12, and inserting a pressure transducer in the tracheal tube/cardiovascular tube.

Measurement of Spinal Acceleration - A Kistler triaxial accelerometer cluster, affixed to thoracic vertebra T12, documented the dynamic response of the spine (Figure 6).

Measurement of Spinal Displacement - Spinal displacement was determined by interpreting the linear displacement of a steel cable attached over the T12 thoracic vertebra triaxial accelerometer cluster (Figure 6). The cable was connected to a gear/pulley that rotated according to a subject's movements during the impact test. The revolutions of the gear were counted by a magnetic pickup probe, and the distance that the spine traveled during the impact was calculated from the probe signal.

Pulmonary Pressure Measurement - As part of the pre-test procedures occurring in the impact laboratory, repressurizing air was introduced via a compressed air reservoir connected by tubing to the tracheal tube. The pulmonary system was repressurized to 15 mm Hg. As illustrated in Figure 4, the tracheal tube is fitted with a pressure-relief valve that opened the pulmonary system to the ambient air just before impact. An Endevco pressure transducer inserted into the tracheal tube measured the pulmonary pressure at initial repressurization and during the changes in pressure throughout the impact.

Abdominal Vascular Pressure Measurement - The cardiovascular system was repressurized as illustrated in Figure 5. A Kulite pressure transducer, guided through the carotid artery tube and positioned in the descending aorta just below the diaphragm, monitored both the degree of initial repressurization and the change during impact. As part of the pre-test procedures occurring in the impact laboratory, the repressurizing fluid was introduced via the catheters through a channel in the center of the two occluding balloons. It is critical to thoraco-abdominal impact testing that the liver be fluid-filled before impact.

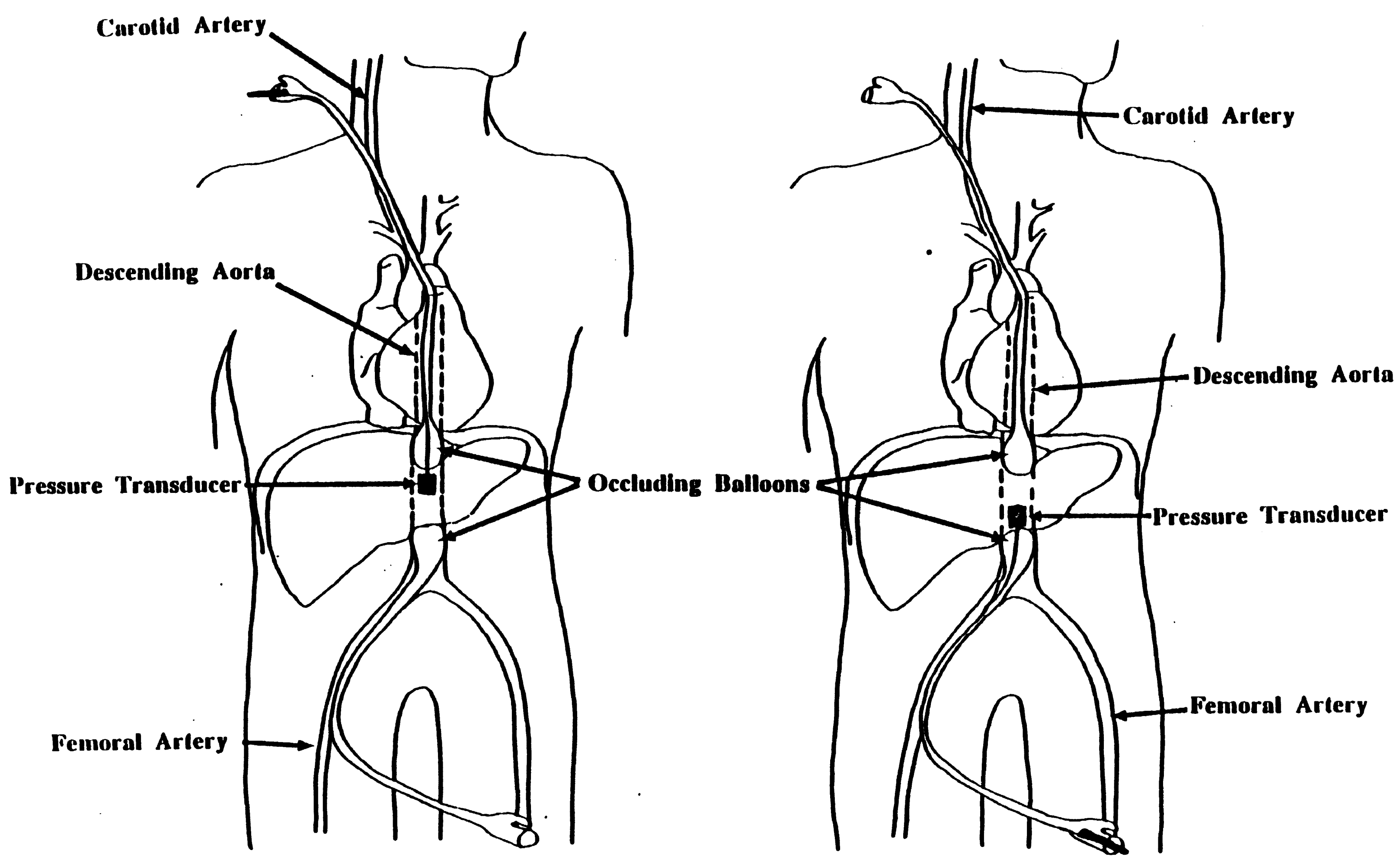

Figure 5. Vascular Repressurization

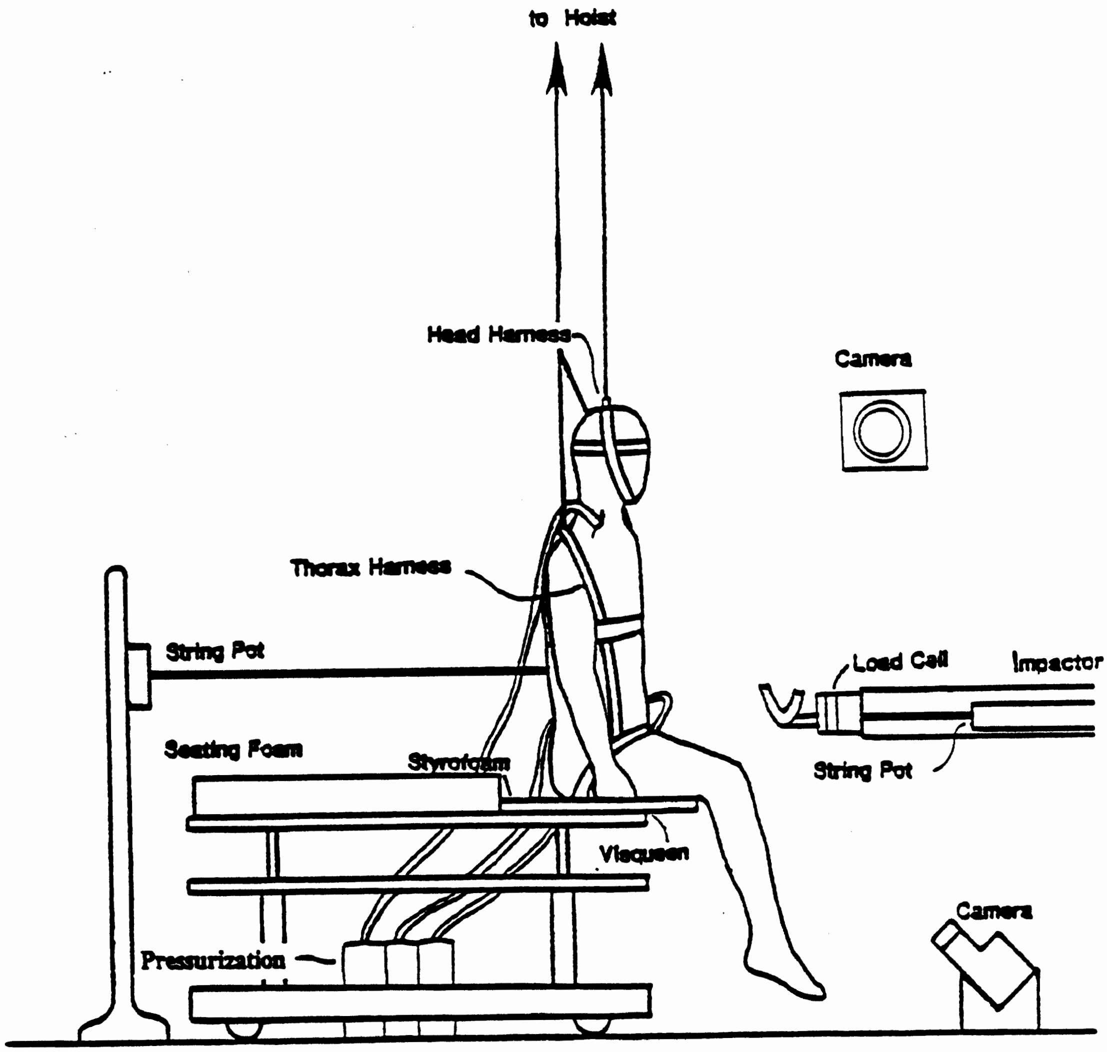

Figure 6. Test Set Up

This was accomplished by pressurizing the area between the two occluding balloons above normal physiological pressure. One to two minutes before impact, the pressure was pulsed between 100-200 mm Hg. Immediately prior to impact, the pressure was dropped to 70 mm Hg.

1.3 Impact Testing

In the impact laboratory, the accelerometers, pressure transducers, and photo targets were attached to subjects. Subject instrumentation included a triaxial accelerometer rigidly affixed to thoracic vertebra T12, a magnetic digital displacement transducer cable attached to the same location, a pressure transducer inserted into the pulmonary tube within the trachea, and a pressure transducer inserted through the cardiovascular repressurization tube into the abdomen.

The impact tests were controlled with an electronic timing device. The impacting device used was the UMTRI pneumatic ballistic pendulum fitted with the model of a rigid lower rim of a steering wheel. Each subject received multiple low-velocity impacts. Five of the seven subjects also received one high-velocity impact. Table 1 summarizes the test design. Gross body motion during impact was recorded by a Hycam camera positioned to film a lateral view of the target area on 16 mm film at 500 (low-velocity testing) and 1000 (high-velocity testing) frames per second.

Contact Region - As illustrated in Figure 6, each subject was placed in a seated position on a mobile, adjustable-height platform covered with friction-reducing clear sheets of plastic, and supported from a ceiling hoist with the head and torso harnesses. The "steering wheel" was positioned to impact a specific contact region on a subject. For example, the **abdomen contact region** was halfway between the most inferior point on rib 10 and the iliac crest; the **rib 10 contact region** was at the most inferior point of rib 10; and the **below sternum contact region** was 1.0 cm below the zyphoid process.

Dynamic Variables and Injury Assessment - After impact testing, each subject was examined for induced injury by means of a gross pathological investigation. The dynamic variables obtained were steering rim force, impact velocity, pendulum acceleration, spinal acceleration, and pulmonary pressure/abdominal vascular pressure. In addition, velocity and displacement at thoracic vertebra T12 were derived from high-speed photogrammetry and the measurements from a magnetic digital displacement transducer.

2.0 Calculation of Values of the Five Injury Criteria

The techniques used to analyze some of the tests to obtain the parameters needed for calculating values for the five injury criteria (Deflection, Viscous, $V_{max}C_{max}$, Specific Absorbed Energy, and Spinal Acceleration) are outlined below. Further detail can be found in references 1-4, 6-10, and 12. Because of limited funds, only the high-velocity tests plus one low-velocity test were used to compute values for the five injury criteria.

2.1 Definitions of the Injury Criteria Variables - This analysis utilized the definition of an injury criterion proposed by Lau and Viano: [11] ***"An injury criterion can be defined as a biomechanical index of exposure severity which, by its magnitude, indicates the potential for impact induced injury"*** [p. 123].

(1) The Deflection Criterion is based on the relative displacement between the spine and the impactor during impact.

(2) The Viscous Criterion is based on the product of the relative displacement of the spine and the impactor, and the velocity associated with that relative displacement. The viscous response is a time function formed by the product of the normalized deflection and the velocity associated with that deflection.

(3) The $V_{max}C_{max}$ Criterion is based on the product of the maximum impact velocity and the maximum relative displacement of the spine and the impactor. $V_{max}C_{max}$ is the product of the maximum of the impact velocity time-history and the maximum of the normalized deflection time-history.

(4) The Specific Absorbed Energy Criterion (SAE) is based on the energy transferred to the thorax and is defined as:

$$SAE = [m_{c35} * m_p/(m_{c35} + m_p)]V_i^2 \qquad (1)$$

where m_{c35} is 35% of the mass of a subject, m_p is the pendulum mass, m_c is a subject's mass, and V_i is the impact velocity, as described by Eppinger and Marcus [10].

(5) The Spinal Acceleration Criterion is based on the resulting acceleration. The spinal-acceleration response is the resulting spinal acceleration measured at thoracic vertebra T12.

Additional Variables - Each dynamic parameter associated with an injury criterion represents, to some degree, one or more aspects of the energy flow and/or management of that energy. In particular, some of the mechanisms of injury associated with some of the injury criteria, e.g, the Viscous Criteria and the Specific Absorbed Energy Criteria, are based upon **energy transferred** to, or **energy absorbed** by, a test subject. Assuming that the injuries produced during impact are related to the energy absorbed by a test subject [1, 10], it is reasonable to compute a quantity such as Energy Loss which represents the total energy absorbed by a test subject at the end of impact. This quantity differs to some degree from the Absorbed Energy Criterion defined by Eppinger and Marcus [10], but is similar to that defined by Lau, Horsch, Viano and Andrzejak [1]. Therefore, in addition to the five injury criteria variables, three other variables were computed: Energy Loss, [V*D]max, and $V_{max}D_{max}$.

(6) Transferred thoracic energy loss (EL) was determined through the use of mechanical impedance (Z), which relates the force at a given point and resulting velocity of a remote point. Analysis of the low frequency components of the mechanical transfer impedance data for the spinal principal-direction acceleration was used to determine the **effective** mass of the thoraco-abdomen system (m_e). The energy loss during impact was then calculated as:

$$EL = 1/2\, m_p (V_i^2 - V_f^2) - 1/2\, m_e v_t^2 \qquad (2)$$

where V_i is the initial velocity of the pendulum and V_f and V_t are the post-impact velocities of the pendulum and thorax respectively determined at the time when impact force has decreased to 50% of its peak value.

Although the deflection used for the Viscous Criterion [1] and for the $V_{max}C_{max}$ Criterion [13] is normalized deflection, it is reasonable to examine the respective un-normalized equivalent variables [V*D]max and $V_{max}D_{max}$ since, to date, there is no clear indication that the normalized variables are better than their un-normalized equivalents.

(7) [V*D]max is the maximum value of the product of the deflection and the velocity of that deflection.

(8) $V_{max}D_{max}$ is the product of the maximum velocity and the maximum deflection.

2.2 Parameters for Injury Criteria Values - It turned out that the parameters needed to calculate values for the five injury criteria included dynamic and descriptive ones. The dynamic parameters needed to calculate values for the five injury criteria are peak force, acceleration, velocity, and displacement of the spine, velocity of the pendulum, normalized deflection (Viscous Criterion formula), normalized deflection ($V_{max}C_{max}$ Criterion formula), and their un-normalized equivalent variables--[V*D]max and $V_{max}D_{max}$. The descriptive parameters needed to calculate values for the five injury criteria are the effective mass of the thoraco-abdomen, 35% of subject mass, and pendulum mass.

Acceleration, Displacement, and Velocity Parameters - Displacement and velocity of the spine and pendulum were obtained from the principal-direction acceleration using the concept of a moving frame, which is briefly outlined in Appendix A. For a more in-depth discussion of the moving frame concept, see references 8, 9, and 12. The displacement and velocity of the spine and pendulum then were used to compute the deflection of the spine at thoracic vertebra T12, as well as the velocity associated with that deflection.

During impact, the acceleration response of the spine manifests itself, primarily, as a change in speed as opposed to a change in direction. The tangential acceleration is the rate of change of speed of the velocity, i.e., the rate of change of the resultant velocity.

Therefore, even though the motion of a given point on the thoraco-abdomen, such as thoracic vertebra T12, is three-dimensional to some degree, the best one-dimensional estimate of that motion is obtained through the use of the tangential acceleration. This approximation can be used when all six degrees of freedom (i.e., three translations and three rotations) are available, as they are when nine or more accelerometers are used. However, a good estimate of the tangential acceleration can be obtained through the use of the principal-direction acceleration when, as in this project, only the data from a triaxial accelerometer cluster are available.

The one-dimensional estimate of the tangential acceleration is then used in conjunction with the film displacement data and digital displacement transducer data to ensure accurate determination of acceleration, displacement, and velocity of a given point on the thoraco-abdomen such as T12. In general, the acceleration of such a point on the thoraco-abdomen cannot be obtained to an acceptable degree of accuracy from either film displacement or magnetic digital transducer displacement data. Similarly, the displacement of such a point generally cannot be obtained from the principal-direction acceleration because of the low-frequency noise in the signals. However, a high-pass filter can be used to help eliminate this low frequency noise so that double integration of the principal-direction acceleration produces displacement data that match the film displacement data to an acceptable level of accuracy.

Yet, in half of the cases presented in this report, it was necessary to compensate the acceleration time-histories for the last 1/3 to 1/2 of the impact duration by scaling with the ratio of the difference between the accelerometer displacement values and the film displacement values so that the film displacement data were matched appropriately. This is done by performing a double integration of the principal-direction acceleration and comparing the result to the spinal displacement obtained from the high-speed film. When the doubly-integrated acceleration begins to diverge from the displacement value obtained from the high-speed film, a rotation of the principal-direction acceleration triad is initiated. The rotation of the principal-direction unit vector is in the plane of the principal and secondary direction so that the doubly-integrated principal-direction spinal acceleration matches the spinal displacement results obtained from the high-speed film.

The one-dimensional estimate of the tangential acceleration is used in conjunction with the film displacement data and digital displacement transducer data to ensure accurate determination of the velocity of a given point on the thoraco-abdomen such as T12. Velocity of the spine and velocity of the pendulum were obtained from an integration of the adjusted principal-direction accelerations.

III. RESULTS

1.0 Significant Results

The significant results are presented in Tables 2-5 in summary form. It is not possible to use these results to evaluate which of the injury criteria are better indicators of abdominal injury because of the different impact contact regions, impact velocities, and multiple impact testing used in this study. When the test protocol was designed, it was assumed that multiple low-velocity impacts would not cause injury to a subject. Table 2 summarizes the testing per subject showing that impact to the lower sternum at low-velocities can cause injuries to the liver. This result implies that any attempt to correlate the observed injuries to the high-velocity impacts would lead to erroneous conclusions. Table 2 shows that it was difficult to injure the liver/spleen by impacting the "soft" abdomen region between the bottom of the 10th rib and the top of the iliac crest, and that it was easier to injure the liver/spleen by impacting the thoracic cage lying over these organs.

2.0 Dynamic Parameters

Table 3 summarizes the dynamic response associated with the injury criteria for the high-velocity impacts and one low-velocity impact. Injury production in an impact environment is a function of many factors. Each dynamic variable associated with the injury criteria represents, in a one-dimensional sense, some aspect of the amount of energy transferred to a test subject. In addition to the five injury criteria variables--the Deflection Criterion, Viscous Criterion, $V_{max}C_{max}$ Criterion, Specific Absorbed Energy Criterion, and Spinal Acceleration Criterion, three other variables are included: Energy Loss, [V*D]max, and $V_{max}D_{max}$.

<u>Obtaining the Dynamic Parameters</u> - For all the tests used for this analysis, the pendulum displacements obtained from the doubly-integrated pendulum principal-direction accelerations matched those of the pendulum film displacement data and those of the pendulum magnetic digital transducer data without the use of the principal-direction rotation

Table 2: Test Summary
86M001

Subject Parameters	Initial Conditions	Velocity m/s	Peak Force N	Peak Force Duration ms
Male, 63 years	Series A	2.5	1400	115
Wt. 70.1 kg	Abdomen	2.5	1400	115
Ht. 180 cm	unpressurized	2.5	1500	115
Cause of Death:		2.5	1300	130
prostate cancer [6]				
	Series B	2.5	1600	140
	Rib 10	2.5	1300	150
	unpressurized	2.5	1700	120
	Series C	2.5	1900	125
	Below Sternum	2.5	2000	120
	unpressurized	2.5	1800	120
	Series D	2.5	1300	135
	Below Sternum	2.5	1500	100
	unrepressurized	2.5	1000	120
		2.5	1300	130
		2.5	1500	130
	Series A	2.5	1250	130
	Abdomen	2.5	1100	120
	unrepressurized	2.5	1100	120
	Series H	10	8900	120
	Abdomen			
	unrepressurized			

Injuries: Stripped contusion on both lungs, lateral to anterior, from Ribs 4-9. Costosternal fracture of right first rib. Ribs 7-10 fractured bilaterally at costochondral junction and 7-12 cm lateral of costochondral junction. Rupture through anterior right lobe of liver. Crushed posterior tip of right lobe of liver. Contused posterior tip of right kidney.

Table 2 (continued)
86M010

Subject Parameters	Initial Conditions	Velocity m/s	Peak Force N	Peak Force Duration ms
Female, 52 years	Series A	2	450	110
Wt. 40.2 kg	Abdomen	2	450	110
Ht. 168 cm	unrepressurized	2.5	580	110
Cause of Death:		2	1100	110
lung cancer		2	1300	110
		2	1300	110
	Series C	2	1650	110
	Below Sternum	2	1650	110
	unrepressurized	2	2050	110
		2	1650	110
	Series E	2	1700	110
	Below Sternum	2	1800	110
	repressurized	2	1600	120
	cardiovascular &	2	1650	110
	pulmonary	2	1650	96
	Series A	2	1900	110
	Abdomen	2	1650	110
	unrepressurized	2.5	1600	110
	Series F	2	1400	110
	Abdomen	2	1500	120
	repressurized	2.5	1550	110
	cardiovascular			
	Series I	6.5	5300	90
	Abdomen			
	repressurized cardiovascular			
	repressurized pulmonary			

Injuries: Right Rib 9 fractured at costochondral jucntion. Rib 10 fractured bilaterally at costochondral junction. Lacerated inferfior vena cava near diaphragm. Torn connective tissue between liver and diaphragm near inferfior vena cava. Crushed liver near entrance of portal vein. Contused stomach.

Table 2 (continued)
86M020

Subject Parameters	Initial Conditions	Velocity m/s	Peak Force N	Peak Force Duration ms
Female, 44 years	Series A	3	--	--
Wt. 57.5 kg	Abdomen	3	1900	110
Ht. 165 cm	unrepressurized	3	2300	120
Cause of Death:		3	2200	110
Hodgkin's Disease				
	Series C	3	2200	90
	Below Sternum	3	2400	90
	unrepressurized	3	2450	90
	Series D	3	2050	90
	Below Sternum	2.4	2050	90
	repressurized	3	1900	90
	pulmonary			
	Series E	3	2400	100
	Below Sternum	3	2450	100
	repressurized			
	cardiovascular &			
	pulmonary			
	Series F	3	2300	120
	Abdomen			
	repressurized			
	cardiovascular			
	Series I	7.5	6700	90
	Abdomen			
	repressurized cardiovascular			
	cardiovascular			

Injuries: Left Rib 8 fracture near costochondral junction. Right Rib 8 displaced fracture near costochondral junction. Lacerated diaphragm--left dome. Bruised jejunum towards the left side. Laceration of anterior left lobe of liver. Superior subcapsulary contusion of left kidney.

Table 2 (continued)
86M030

Subject Parameters	Initial Conditions	Velocity m/s	Peak Force N	Peak Force Duration ms
Female, 60 years	Series A	3	2200	80
Wt. 47.0 kg	Abdomen	3	2300	90
Ht. 166 cm	unrepresssurized	3	2500	80
Cause of Death:		3	2500	85
brain aneurysm				
	Series C	1.3	220	80
	Below Sternum	2	--	--
	unrepressurized	2	1600	80
		3	1700	80
	Series D	2	1500	80
	Below Sternum	2	1500	80
	repressurized	2	1600	80
	pulmonary			
	Series E	2	1300	80
	Below Sternum	2	1500	80
	repressurized	2	1400	85
	cardiovascular &			
	pulmonary			
	Series G	2	1300	100
	Abdomen	2	1300	100
	cardiovascular &	2.5	1400	100
	pulmonary			
	No Series H or Series I			
	high-velocity impact			

Injuries: Contusion in musculature over lower sternum. Bilateral contused musculature overlying Ribs 10-12. Superficial laceration of lateral surfaceof inferior lobe of left lung. Rib 6 fractured bilaterally near costochondral junction. Superficial laceration of anterior left lobe of liver.

Table 2 (continued)
86M040

Subject Parameters	Initial Conditions	Velocity m/s	Peak Force N	Peak Force Duration ms
Male, 46 years	Series G	2.4	1400	90
Wt. 50.0 kg	Abdomen	3	1600	90
Ht. 176 cm	repressurized	3	1300	100
Cause of Death:	cardiovascular	3	1100	110
cancer	repressurized	3	1250	110
	pulmonary	3	1200	110
	Series I Abdomen repressurized cardiovascular repressurized pulmonary	10.8	8450	50

Injuries: Superficial laceration of superior left lobe of liver.

Table 2 (continued)
86M050

Subject Parameters	Initial Conditions	Velocity m/s	Peak Force N	Peak Force Duration ms
Female, 55 years Wt. 70.3 kg Ht. 162 cm Cause of Death: cancer	Series G Abdomen repressurized cardiovascular repressurized pulmonary	-- 3 3 3	-- 1200 1200 1500	-- 120 110 110
	Series I Abdomen repressurized cardiovascular repressurized pulmonary	9.3	6700	85

Injuries: None

Table 2 (continued)
86M060

Subject Parameters	Initial Conditions	Velocity m/s	Peak Force N	Peak Force Duration ms
Male, 61 years Wt. 61.9 kg Ht. 178 cm Cause of Death: prostate cancer and lung cancer	Series E Below Sternum repressurized cardiovascular pulmonary	2 3.9	1250 3100	140 90
	No Series H or Series I high-velocity impact			

Injuries: Rib 6 fractured bilaterally near costochondral junction. Rib 7 bilateral displaced fracture near costochondral junction. Contused stomach. Medial contusions on both lungs. Contusion posterior surface of inferior lobe of left lung. Contusion inferior lateral surface of superior lobe of left lung. Contusion to quadrate lobe and lateral segment of posterior left lobe of liver. Superficial laceration medial segment of antgerior left lobe of liver.

Table 3

Variables Associated with the Injury Criteria

Test Number	Velocity m/s	Peak Force N	Energy Loss[2] N-m	Specific[1] Absorbed Energy N-m/kg	Peak Spinal Acc. m/s/s	Peak Viscous V*C m/s	Peak Viscous V*D m2/s	Peak Normalized Deflection C %	Peak Deflection D	V_{max} x C_{max} m/s	V_{max} x D_{max} m2/x
86M006	10.0	8900	520	7.42	620	2.34	0.75	53	0.17	5.31	1.70
86M016	6.5	5300	260	4.13	560	1.04	0.25	38	0.09	2.50	0.60
86M026	7.5	6700	320	4.63	400	1.00	0.28	36	0.10	2.68	0.75
86M042	10.8	8400	570	11.02	420	1.69	0.49	48	0.14	5.17	1.50
86M052	9.3	6700	480	6.40	300	1.42	0.44	48	0.15	4.52	1.40
86M062	3.9	3000	140	1.29	170	0.35	0.12	21	0.07	0.79	0.27

[1] Based on ESV procedure [10].

[2] Based on effective mass from mechanical impedance.
Series 000-060: 26, 16, 26, 29, 38, 38, 24 kg.

procedure. However, when the principal-direction spinal acceleration data were compensated by use of the high-speed film spinal displacement data, the doubly integrated spinal acceleration produced results which were similar to both the high-speed spinal displacement film data and the magnetic digital transducer displacement data as shown in Figure 7. The adjusted principal-direction spinal acceleration was only slightly different from the unadjusted principal-direction spinal acceleration (i.e., no rotation was performed), as shown in Figure 8.

Force-Deflection Variability - The force-deflection curves for the high-velocity tests shown in Appendix B represent the responses of the "soft" abdomen for different test subjects at different velocities (Figures 9A and 9B), except for Test 86M062 which is for impact to the sternum. In terms of force-deflection, the tests showed considerably different responses. In general, force-deflection response similarity between tests is greatest for deflections up to 4-5 cm.

Before the test results can be used to characterize the impact response of the abdomen, it is desirable to consider the factors other than subject biovariability that may have caused the observed variability in force-deflection response among tests. These include: 1) off-axis loading of the steering rim load cell, 2) non-linearities in response, 3) pendulum mass relative to a subject's body mass, and 4) three-dimensional motion of the test subjects.

It was decided upon review of the high-speed films that some off-axis loading of the steering wheel rim which would have affected the force-deflection response might have occurred just after the time of maximum force. The effect of potential off-axis loading of the steering rim load cell was evaluated quantitatively in the following manner. As Eppinger and Marcus [10] have proposed, the mass of the thorax was estimated to be 35% of a subject's weight. The product of this mass and the inferior-superior direction spinal acceleration was used to estimate the force perpendicular to the impact direction. This

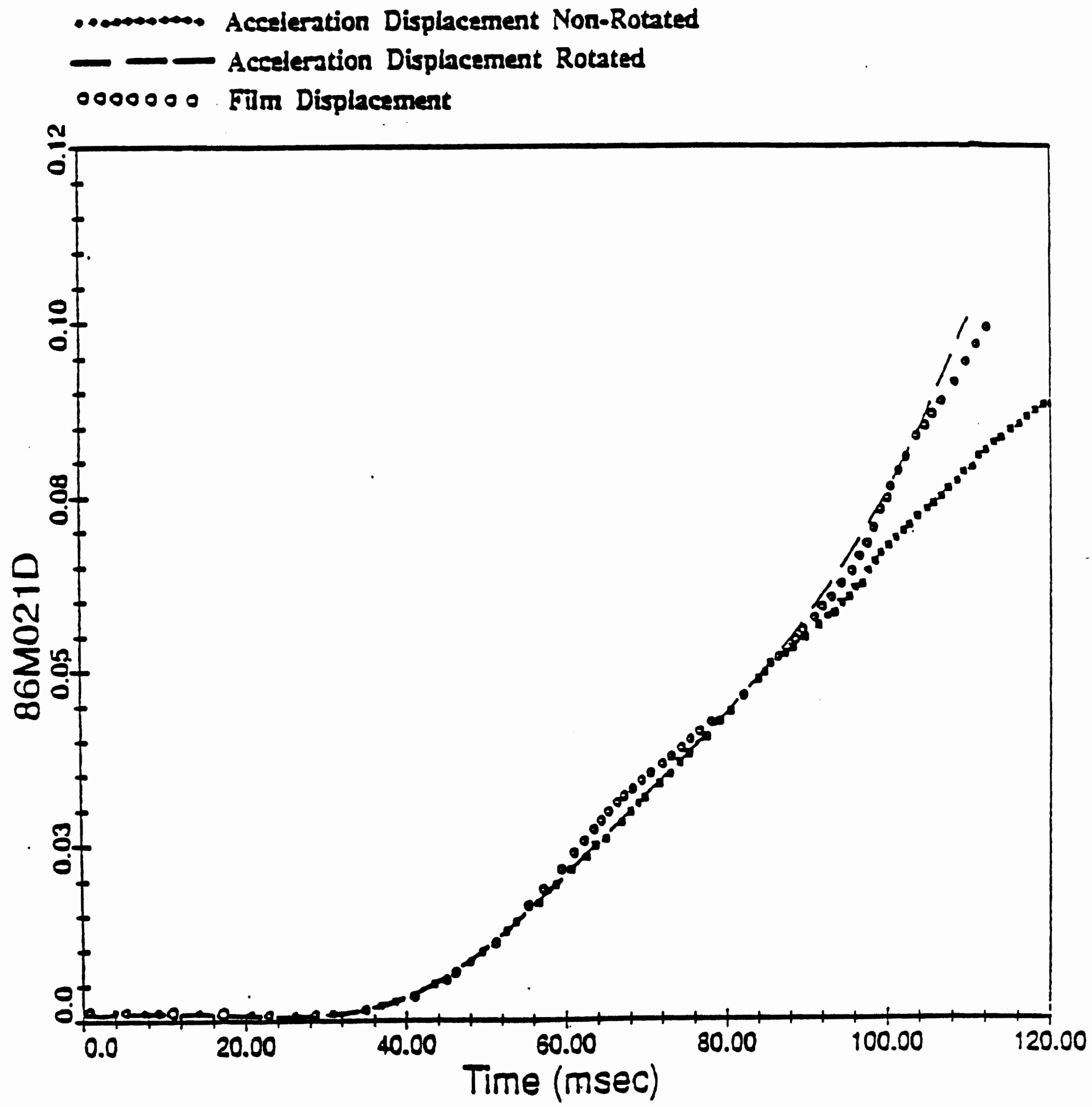

Figure 7. T12 Displacement versus Time for Doubly Integrated Acceleration and Film Data

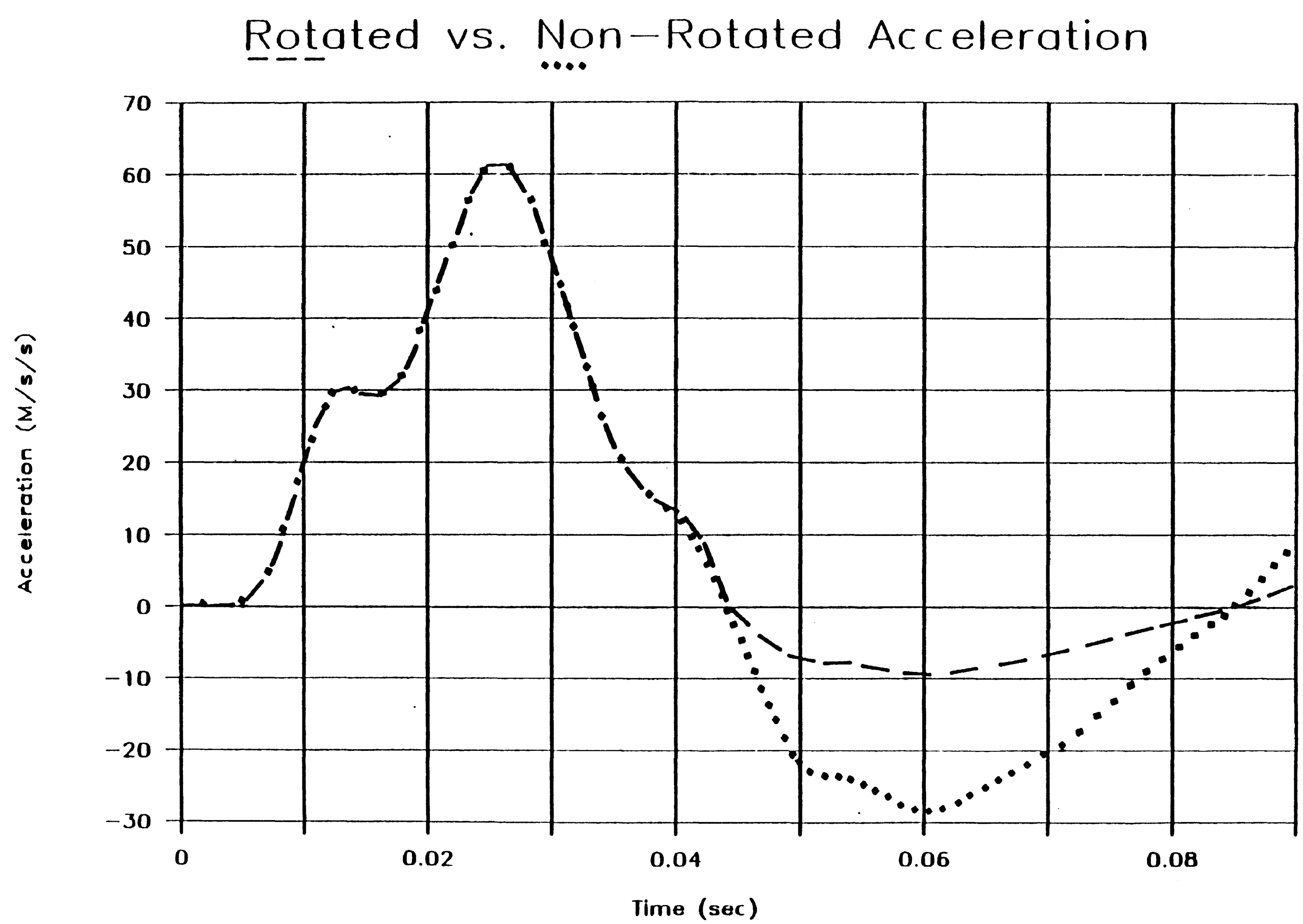

Figure 8. Comparison of Principle Direction Acceleration

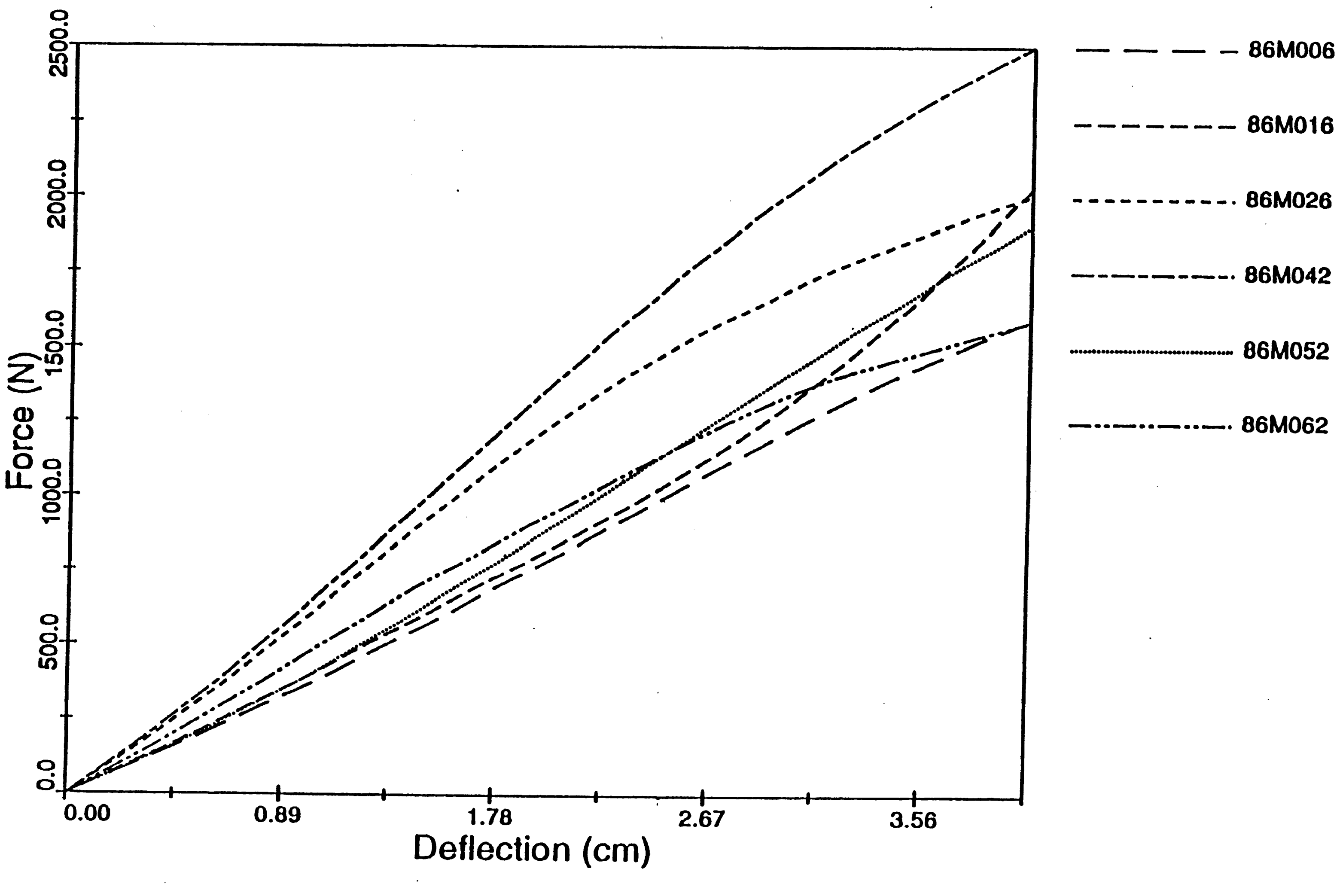

Figure 9A. Comparison of Initial Positions of Force-Deflection Curves for High-Velocity Impacts.

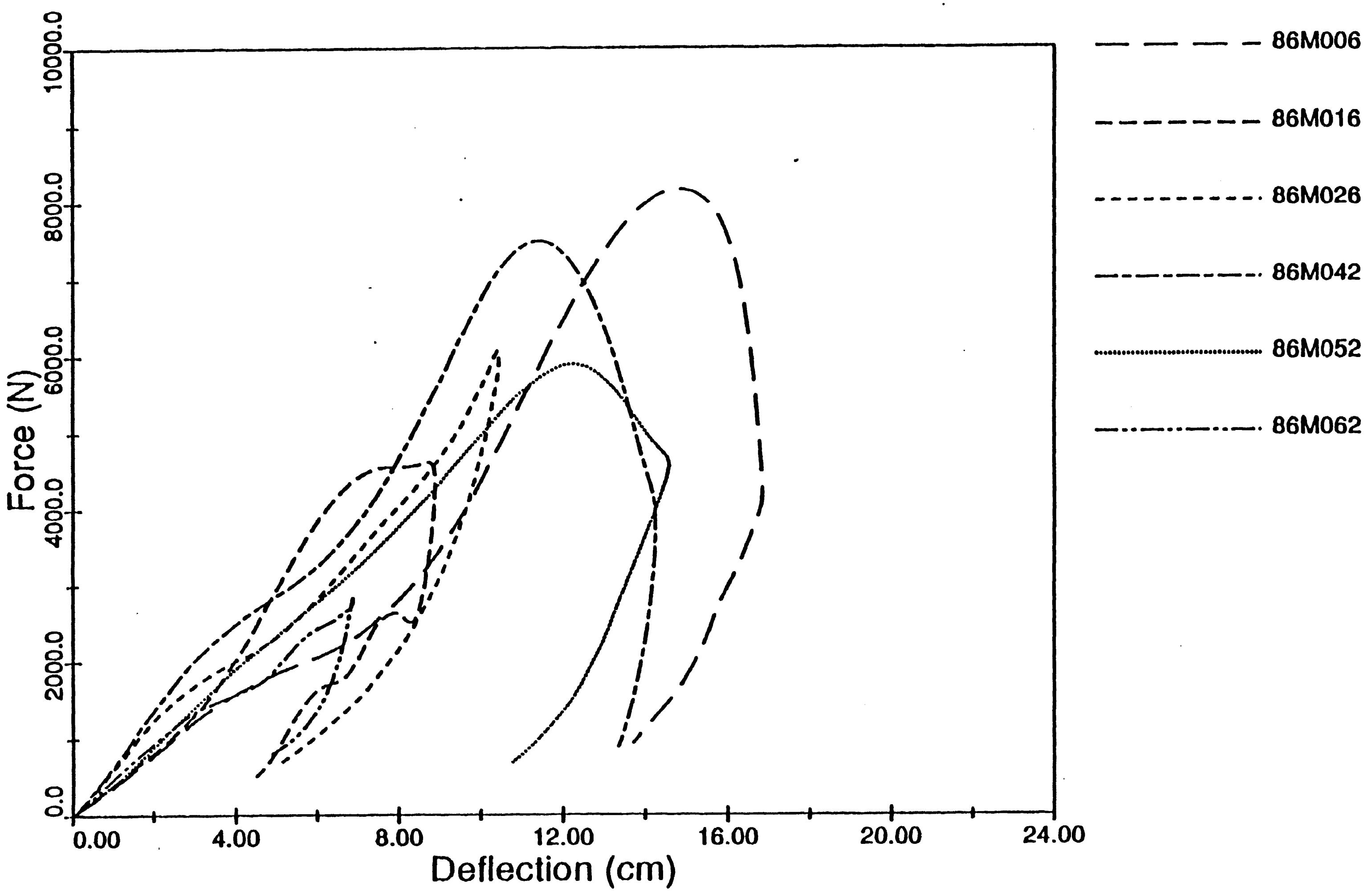

Figure 9B. Comparison of Force-Deflection Curves for High-Velocity Impacts force then was applied to the steering wheel rim, and its effect on the axial force measurement was determined. The results showed that off-axis loading forces would not have exceeded 15% of the actual force value.

Some variability in the force-deflection response may be attributed to non-linearity in the response of the test subjects. For example, consider Figure 10 which represents the force-deflection curve for a high-velocity impact (Test 86M006). The increase in the slope half way between the initiation of impact and peak force may be due to bottoming out of the abdominal tissue against the spine. Note that this is a general trend in which an increase in slope occurs in those tests having higher penetrations of the abdomen. However, Test 86M062 in the Appendix may be an exception to this generalization. If it is true that Test 86M062 is an exception, then the test data show that different levels of penetration produce different impact responses. This is an important consideration for determining the maximum penetration for a given force.

Another factor which could have affected the variability in the response of the subjects was the mass of the pendulum which was only 18 kg. Differences in the effective mass of test subjects would significantly affect the amount and rate of energy transferred to a subject from the pendulum and, therefore, would affect the response. This would have been particularly important, even for a linear system, if that response was rate- or velocity-sensitive.

Three-dimensional motion of the test subjects could have affected the force-deflection responses which are presented in this report as one-dimensional responses. Observations from the high-speed films indicate that this should be an acceptable assumption up to the occurrence of peak force, but during the recovery phase of the force-time histories, a two- or three-dimensional description may be needed.

Before the test results can be pooled to determine a general response, the effects of off-axis loading of the steering wheel load cell, of the non-linearities in response of the

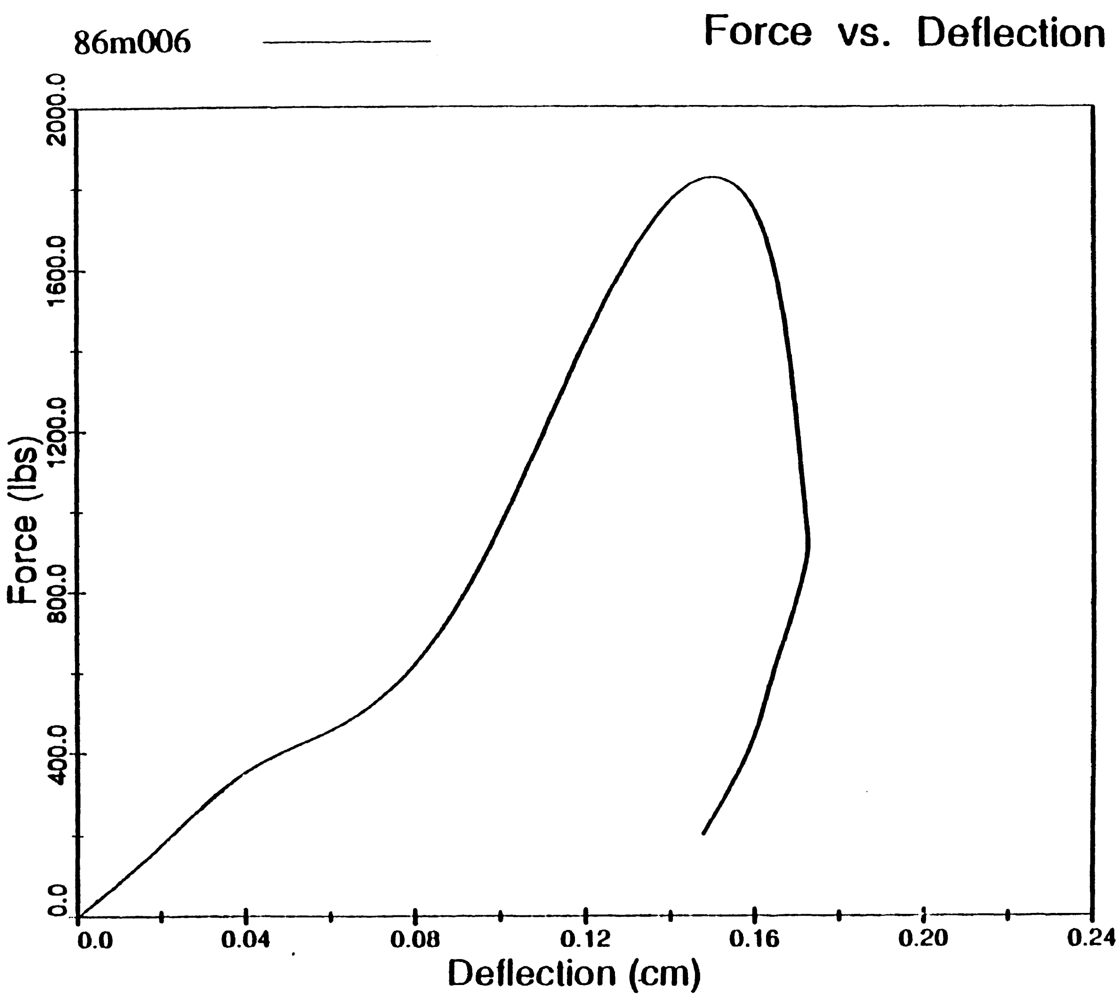

Figure 10. High-Velocity Impact Force-Deflection Curve

Table 4
Correlation Matrix of Variables Associated with the Injury Criteria

VARIABLE	Velocity	Peak Force	Energy Loss	Specific Absorbed Energy	Peak Spinal Acceleration	Peak Viscous $V_{max} \cdot C_{max}$	Peak Viscous $V_{max} \cdot D_{max}$	Peak Normalized Deflection	Peak Deflection	$V_{max} \cdot C_{max}$	$V_{max} \cdot D_{max}$
Velocity	1.0000										
Peak Force	.9588	1.0000									
Energy Loss	.9916	.9341	1.0000								
Specific Absorbed Energy	.9486	.8846	.9463	1.0000							
Peak Spinal Acceleration	.5049	.6522	.4356	.4280	1.0000						
Peak Viscous $V_{max} \cdot C_{max}$	.8917	.9357	.8911	.7885	.7145	1.0000					
Peak Viscous $V_{max} \cdot D_{max}$	.8562	.9020	.8711	.7391	.6323	.9878	1.0000				
Peak Normalized Deflection	.9515	.9287	.9391	.8389	.6482	.9459	.9093	1.0000			
Peak Deflection	.9108	.8847	.9338	.7790	.4688	.9416	.9561	.9446	1.0000		
$V_{max} \cdot C_{max}$	.9841	.9445	.9888	.9128	.5348	.9405	.9184	.9760	.9610	1.0000	
$V_{max} \cdot D_{max}$	.9569	.9224	.9760	.8671	.4752	.9447	.9459	.9541	.9876	.9885	1.0000

Number in a Sample = 6
Degrees of Freedom = 4

Confidence Intervals

P5% = 0.8114
P1% = 0.9172

subjects, of the pendulum mass relative to a subject's body mass, and of the three-dimensional motion of the test subjects need to be quantified. However, it is difficult to separate out how much of the variability in the force-deflection response was due to the factors just mentioned and how much of it was due to the biovariability of the test subjects shown in Table 4 because of the small sample size and the constraints imposed by the limitations of this type of data.

3.0 Relationships Among Injury Criteria Variables

Table 4 summarizes the correlation between the variables associated with the injury criteria values. All of the variables correlated well with each other, except for Peak Spinal Acceleration. This shows that four of the five criteria are based upon similar aspects of the energy transferred to, or absorbed by, a test subject. When the Deflection variable is normalized, then the correlation between Energy Loss and either the $V_{max}C_{max}$ or viscous variables is improved.

4.0 Subject Biovariability

Table 5 summarizes the subject anthropometry. Mean subject weight was 56.7 kg with a standard deviation of 10.7, ranging from 40.70 kg, and mean subject height was 170.8 cm with a standard deviation of 6.8, ranging from 161-180 cm. The mean age was 54.4 years with a standard deviation of 9.3, ranging from 44-63 years. Subject biovariability may be very significant because with only seven test subjects there is a respectable variation in age, weight, and height. In addition, dimorphic effects are probably greater because the sample consisted of three males and four females.

Table 5
Cadaver Anthropometry
(all dimensions in centimeters)

Measurement	Cadaver Number 86M001	86M010	86M020	86M030	86M040	86M050	86M060
Stature	180.0	168.4	164.5	166.0	176.2	161.8	178.4
Weight*	70.1	40.2	57.5	47.0	50.0	70.3	61.9
Head Circumference	58.5	54.0	55.3	58.0	58.8	54.5	55.1
Head Length	19.5	17.2	18.8	19.5	17.1	19.1	19.2
Head Breadth	16.0	15.0	15.2	16.3	15.7	15.6	14.1
Menton-Vertex	22.2	21.7	22.6	24.3	22.7	19.5	21.8
Menton-Suprasternale	11.2	13.2	7.5	5.9	8.6	7.2	9.5
Neck Circumference	34.5	30.0	30.9	32.0	33.0	38.0	33.8
Acromion Height	26.7	22.3	23.9	23.5	23.3	23.2	22.7
Suprasternale Height	33.4	31.3	30.8	30.4	41.4	27.1	31.8
Substernale Height	54.5	49.4	48.7	49.0	49.5	39.3	52.5
Substernale Circumference	93.0	75.0	76.0	87.2	78.5	92.2	90.0
Axillary Breadth	27.2	28.4	26.2	31.0	26.0	28.6	28.7
Chest Breadth	31.0	27.0	25.6	31.2	26.8	30.7	29.7

* kilograms

IV. DISCUSSION

As stated earlier, the focus of this analysis was to develop the tools needed to determine the parameters needed for computation of injury criteria values from the dynamic test data as one means of assisting in the evaluation of the relative predictive abilities of the different **thoracic** criteria for ***abdominal*** trauma. Although it is not possible to relate these injury criteria values to the observed injuries directly, it is possible to evaluate the five criteria in terms of the amount of energy transferred to, or absorbed by, a test subject and with regard to their inherent limitations in representing dynamic parameters and definitions.

1.0 Energy Transferred to, or Absorbed by, a Test Subject

Although in this analysis the injury criteria values cannot be directly related to the observed injuries, analyses made by other researchers of their own data show that there is considerable controversy over which of the five injury criteria is the best indicator of **thoracic** injury. For example, Lau, Horsch, Viano, and Andrzejak [1] believe the Viscous Criterion is the best indicator of thoracic injury; Eppinger and Marcus [10] believe the Specific Absorbed Energy Criterion is the best indicator of thoracic injury; and Kroell, Allen, Warner, and Thomas [13] believe the $V_{max}C_{max}$ Criterion is the best indicator of thoracic injury. Which of these might be the best indicator of **abdominal** injury? The consensus among these researchers seems to be that injury is a function of the energy transferred to, or absorbed by, a test subject during impact. Therefore, it was thought worthwhile in this study to develop a clearer definition of energy flow and to attempt to measure it. The Energy Loss variable, defined in Section II, 2.1, represents an attempt to accomplish the measurement of a clearly defined energy flow to a subject during impact.

For all of the injury criteria, it is assumed that injury is related to the amount of energy transferred to, or absorbed by, a test subject [1, 10, 13]. Each dynamic variable associated with an injury criterion represents, to some degree, one or more aspects of the energy flow and/or management of that energy. For example, deflection represents, to some degree, the work needed to deform the thorax. The Viscous response and the $V_{max}C_{max}$ response represent, to some degree, the energy dissipated during impact. The question becomes which variables represent the energy flow and/or management of that energy in such a way that abdominal injury, or a threshold of abdominal injury, can be predicted accurately.

Close Correlation of Four of the Criteria - The numerical values of the injury criteria variables determined from the current dynamic test data and information were correlated because it was possible to determine to what extent they measured the same aspect of transferred energy. It was determined that all of the variables correlated well with each other, except for Peak Spinal Acceleration, as shown by Table 4. It is expected that since the Viscous, Specific Absorbed Energy, and $V_{max}C_{max}$ responses are representative of the energy loss that they would correlate well with Energy Loss. Yet Peak Force, Deflection, and Impactor Velocity also correlate well with Energy Loss. That these parameters correlate well with each other makes it difficult to determine which of these injury criteria might prove to be superior for this type of testing. If, at some future date, all of these four injury criteria are found to predict abdominal injury successfully, the injury criterion that is "best" might simply be the easiest one to obtain.

2.0 Injuries

2.1 GMRL Steering Wheel Model and Injuries

High-Velocity Impact and Injuries - The first three test subjects received a series of low-velocity impacts followed by one high-velocity test (86M006, 86M0016, and 86M0026). In each case, severe liver injuries occurred. It was hypothesized that the injuries were a result of the high-velocity impact with no aspect related to the low-velocity tests.

Multiple Low-Velocity Impacts and Injuries - It was decided to examine the assumption that the injuries were a result of the high-velocity impact with no aspect related to the multiple low-velocity impacts with subject 86M030. That subject's test series consisted of seventeen low-velocity impacts to different areas of the abdomen, resulting in minor liver injury. No high-velocity impact was conducted.

Low-velocity thoraco-abdominal impacts produced liver injuries. However, this type of steering wheel assembly is extremely damage-producing because of the stiffness of the steering wheel rim, which is consistent with the observations of others [5]. A realistic steering system may not be damage-producing in a 3 m/s low velocity impact.

2.2 Impact Contact Region and Injuries

Given that the liver and spleen are being considered abdominal organs in this analysis, a thoracic contact region is very important for abdominal trauma and an abdominal contact region is less important for abdominal trauma because: 1) it appears difficult to injure the liver by impacting the "soft" abdomen (i.e., the region between the bottom of the 10th rib and the top of the iliac crest), and 2) it seems the impactor must be directly over the liver to produce injury to it. This may also be true for the spleen. Thus, contact region is a very important aspect of abdominal injury production, and, perhaps, may be so even for the "less stiff" deformable-rim steering wheel assemblies. The contribution of contact region may be so important that without taking it into consideration with greater exactitude that is currently done, any accurate determination of the success of an injury criterion for the abdominal region or for organs such as the liver and spleen is difficult.

Sternum versus Abdomen Contact Region and Injuries - In consideration of these results, it was proposed that impact to the lower sternum at low-velocity could cause injuries to the liver. To evaluate this hypothesis, three subjects were tested: one subject was impacted at low-velocity (3.9 ms) at the sternum, producing minor liver injuries;

another subject, impacted six times at low-velocity (3 ms) and once at high-velocity (11 ms) at the abdomen, had similar liver injuries, while the next subject, impacted six times at low-velocity (3 ms) and once at high-velocity (9 ms) at the abdomen, had no injury. As stated previously the result was that it appears difficult to injure the liver by impacting the "soft" abdomen (i.e., the region between the bottom of the 10th rib and the top of the iliac crest) and it seems that the impactor must be directly over the liver to injure it.

3.0 Inherent Limitations of the Five Criteria

Although it is not possible to evaluate which of the injury criteria are better indicators of abdominal injury because of the different impact contact regions, multiple impact testing, and impact velocities used in this study, some inferences can be drawn from the analysis of these data.

Spinal Acceleration is Not an Indicator of Abdominal Injury - The Spinal Acceleration Criterion predicts injury at the 60 g level. Most of the injuries observed in these tests occurred well below the 60 g level: in only one test did the spinal acceleration exceed 60 g. Therefore, it is most likely that, even if the observed injuries cannot be related directly to the five criteria, the Spinal Acceleration Criterion is not a good indicator for abdominal/liver or other soft tissue injury. This idea is further supported by the poor correlations of spinal accelerations with other potential injury criteria such as velocity, force, and absorbed energy (see Table 4).

Injury Scoring Ambiguities - Following the assumption of Lau, Horsch, Viano and Andrzejak [1] that the liver and spleen are part of the abdomen because of their anatomical location beneath the diaphragm, this analysis considered the liver and spleen to be abdominal organs. (However, the liver and spleen had been considered part of the thorax because of their partial housing within the thoracic cage [3, 10].) This means that the same dynamic results and test information involved in computing a value for each of the five injury criteria could be scored as being associated with either a presence or an absence of injury. For example, if the only observed injury is a severely injured liver and the liver is defined as an **abdominal** organ, then a criterion would be associated with an absence of thoracic trauma. This would be the same for all the values computed for the five injury criteria; they would be associated with lethal liver injuries scored as "no injury" if the liver were perceived to be an abdominal organ. On the other hand, if the only injury is a severely injured liver and the liver is defined as a **thoracic** organ, then a criterion would be associated with the presence of thoracic trauma and scored as "severe injury." Moreover, lumping injuries to obtain an overall score for a body region such as the thoraco-abdomen (i.e., body trunk) does not wholly eliminate this problem. In addition, there is a grave potential for ambiguity of interpretation when injury criteria values are matched to lumped injuries, such as a calculation of an overall AIS for a smaller body region such as the thorax or abdomen [13, 14] and contrasted to injury criteria values which are matched to unlumped injuries, such as a calculation of an AIS for one organ like the liver [1]. Those who favor overall scores for a body region recognize the problems in scoring multiple less-severe injuries versus single severe injuries; for example, Kroell, Allen, Warner, and Perl [13] included both types of information in their report findings.

Effect of Impact Contact Region - In order to choose one of the injury criteria over any of the others as having greater predictive ability for abdominal injury, one must be able to show that the "selected criterion" correlates better with abdominal injury than the others. However, nowhere in the computation of each of the injury criteria response functions is there any consideration of the effect of contact region. Yet based on these test data it would seem that one can greatly reduce/increase abdominal injury by changing contact region or definitions of the liver/spleen as ***abdominal*** or ***thoracic*** organs.

V. CONCLUSIONS

This was a limited study of the impact and injury response of the abdomen used to develop procedures and techniques necessary for computation of values for five **thoracic** injury criteria from dynamic laboratory data and test information as one means of assisting in the evaluation of these criteria for abdominal trauma. Values were calculated for the Deflection Criterion, Viscous Criterion, $V_{max}C_{max}$ Criterion, Specific Absorbed Energy Criterion, and Spinal Acceleration Criterion. The experiments utilized special impact conditions, for example, an idealized rigid lower one-third of a steering wheel rim was used as the impact surface and multiple impacts were conducted. The results and conclusions presented apply only to a limited analysis of the test data. More analysis of the data needs to be performed before general conclusions about the kinematic response of the thoraco-abdomen can be drawn. In addition, more tests need to be performed before general conclusions about the abdominal injury predictive capabilities of four of the five injury criteria can be drawn. However, the following limited conclusions can be drawn:

1. The kinematic variables associated with the five injury criteria can be calculated from data obtained from triaxial accelerometers in conjunction with electromechanical displacement transducers and the photogrammetry of high-speed films.

2. The Spinal Acceleration Criterion must be altered in order to be a predictor for abdominal trauma, because as it is currently formulated, it is not a good indicator of abdominal or liver trauma.

3. The contribution of impact contact region may be so important for injury production that not taking it into consideration would make any determination of the predictive accuracy of these injury criteria extremely difficult.

4. In the experiments presented here, ranging in velocity from 4 to 12 m/s, there is no important difference in the force-deflection curves for the first 4 cm of penetration. This implies that the initial response of the abdomen is not impact-velocity dependent.

5. The stiffness of the steering rim is an important factor in injury production.

VI. FUTURE WORK

The original goal of the testing was to use the thoraco-abdominal impact testing protocols which had been designed in 1985-1986 to evaluate the effects of different conditions on the impact/injury response of the abdominal region of the unembalmed cadaver surrogate. In particular, the tasks were to investigate the effects of vascular repressurization of the abdominal cavity, pulmonary repressurization, impact contact region on the injuries produced, and the effect of the repeatability of the results from the cadaver surrogates, as well as to provide information for comparison of the impact response of the repressurized cadaver surrogate to that of the porcine surrogate experiments of Lau, Horsch, Viano, and Andrzejak [1]. The analysis of the data will continue and the report for Project 8131 (1987-1988) will present an evaluation of these different conditions on the impact response of the abdominal region of the unembalmed cadaver. In addition, a further assessment of the five injury criteria will be made.

VII. REFERENCES

1. Lau, I.V., Horsch, J.D., Viano, D.C., and Andrzejak, D.V. 1987. Biomechanics of Liver Injury by Steering Wheel Loading. Journal of Trauma 27(3), pp. 225-235.

2. Nusholtz, G.S., Kaiker, P.S., and Bosio, A.C. 1985. Thoracic Response to Frontal Impact. 29th Stapp Car Crash Conference Proceedings, pp. 17-48.

3. Nusholtz, G.S., Kaiker, P.S., Huelke, D.F., and Suggitt, B.R. 1985. Thoraco-Abdominal Response to Steering Wheel Impacts. 29th Stapp Car Crash Conference Proceedings, pp. 221-267. SAE Paper No. 851737.

4. Harris, C.M. and Crede, C.E. 1976. Shock and Vibration Handbook. New York: McGraw-Hill Book Co.

5. Horsch, J.D., Lau, I.V., Viano, D.C., and Andrzejak, D.V. 1985. Mechanism of Abdominal Injury by Steering Wheel Loading. 29th Stapp Car Crash Conference Proceedings, pp. 69-78.

6. Nusholtz, G.S. 1986. Steering Wheel Abdominal Impact Trauma. MVMA Project No. 6131 Final Report. The University of Michigan Transportation Research Institute, Ann Arbor, Michigan.

7. Nusholtz, G.S., Melvin, J.W. and Alem, N.M. 1979. Head Impact Response Comparisons of Human Surrogates. 23rd Stapp Car Crash Conference Proceedings, pp. 497-541. SAE Paper No. 791020.

8. Nusholtz, G.S., Melvin, J.W., Huelke, D.F., Alem, N.M. and Blank, J.G. 1981. Response of the Cervical Spine to Superior-Inferior Head Impact. 25th Stapp Car Crash Conference Proceedings, pp. 197-237. SAE Paper No. 811005.

9. Nusholtz, G.S., Melvin, J.W., and Lux, P. 1983. The Influence of Impact Energy and Direction on Thoracic Response. 27th Stapp Car Crash Conference Proceedings, pp. 69-94. SAE Paper No. 831606.

10. Eppinger, R.H. and Marcus, J. 1985. Production of Injury in Blunt Frontal Impact. 10th International Conference on Experimental Safety Vehicles Proceedings. U.S. Department of Transportation, National Highway Traffic Safety Administration, pp. 90-104.

11. Lau, I.V. and Viano, D.C. 1986. The Viscous Criterion--Bases and Applications of an Injury Severity Index for Soft Tissues. 30th Stapp Car Crash Conference Proceedings, pp. 123-142. SAE Paper No. 861882.

12. Spivak, M. 1979. A Comprehensive Introduction to Differential Geometry, Second Edition, Volume II, Berkeley, CA: Publish or Perish, Inc.

13. Kroell, C.K., Allen, S.D., Warner, C.Y. and Perl, T.R. 1986. Interrelationship of Velocity and Chest Compression in Blunt Thoracic Impact to Swine II. 30th Stapp Car Crash Conference Proceedings, pp. 99-122. SAE Paper No. 861881.

14. Stalnaker, R.L. and Ulman, M.S. 1985. Abdominal Trauma-Review, Response, and Criteria. 29th Stapp Car Crash Conference Proceedings, pp. 1-16. SAE Paper No. 851720.

APPENDICES

APPENDIX A: Moving Frames and Frame Fields

As the thoraco-abdomen moves following impact through space, any point on it generates a trajectory or path in space that is a function of time and velocity. A vector field is a function which assigns a uniquely defined vector to each point along such a path. Any three mutually orthogonal unit vectors defined on a path are a frame field. Any vector, such as the acceleration vector, defined on a path may be resolved into three orthogonal components of any well-defined frame field, such as a laboratory or anatomical frame field. Changes in a frame field over time (e.g. the angular velocity of the frame field) can be resolved into three components and are then expressible in a dual frame field for analysis.

Other frame fields, such as the **Frenet-Serret Frame** [4, 8, 9], which contain information about the motion embedded in the frame field, are also useful for describing the motion caused by blunt thoraco-abdominal impact. The three orthogonal unit vectors $(\hat{T}, \hat{N}, \hat{B})$ shown in Figure A1 form a right-handed triad, called the Frenet-Serret triad, at each point along the space curve. The collection of these triads along a given curve is known as a Frenet-Serret frame field, which is stationary in three-dimensional space. The turning and twisting of a space curve generated by a moving point can be described in terms of curvature, κ, and torsion, τ. Curvature, in terms of the Frenet-Serret triad, is defined as:

$$N\kappa = d\hat{T}/ds$$

while the torsion is given by:

$$N\tau = - d\hat{B}/ds.$$

The rates of change of $(\hat{T}, \hat{N}, \hat{B})$ with respect to time may be obtained from the following relations:

(T-rate) $d\hat{T}/sr = -\kappa VN, dN/dt = -\kappa VT + \kappa V\hat{B}$, and

(B-rate) $d\hat{B}/dt = - \kappa V\hat{N}$.

Thus, the turning and twisting of a space curve and the rates of turning and twisting are described by the Frenet-Serret triad ($\hat{T}$, $\hat{N}$, $\hat{B}$).

In the case of a single triaxial accelerometer, the use of the Frenet-Serret frame is impossible, but it has been found [4, 8, 9] that in many cases during direct impacts it is possible to find an approximation to the Frenet-Serret frame. This is done by finding the most significant component of acceleration, and, therefore, the principal direction of motion. One method of determining the principal direction of motion and constructing the **Principal Direction Triad** was to determine the direction of the acceleration vector in the moving frame of the triaxial accelerometer cluster and then describe the transformation necessary to obtain a new moving frame that would have one of its axes in the principal direction. A single point in time at which the acceleration was a maximum was chosen to define the directional cosines for transforming from the triax frame to a new frame in such a way that the resultant acceleration vector (AR) and principal unit vector (A1) were co-directional. This then was used to construct a new frame rigidly fixed to the triaxial accelerometer cluster, but differing from the original one by an initial rotation. After completing the necessary transformation, a comparison among the magnitudes of the approximations of the principal direction acceleration and the resultant acceleration was performed.

The second rotation was used to find the secondary direction which is an approximation of the normal acceleration. First, the most significant component of acceleration in the plane perpendicular to the principal direction was determined in a manner similar to that used for finding the principal direction acceleration in three directions. The tertiary direction which fills out the principal direction triad was then the cross product of the principal and second direction accelerations.

APPENDIX B: Plots

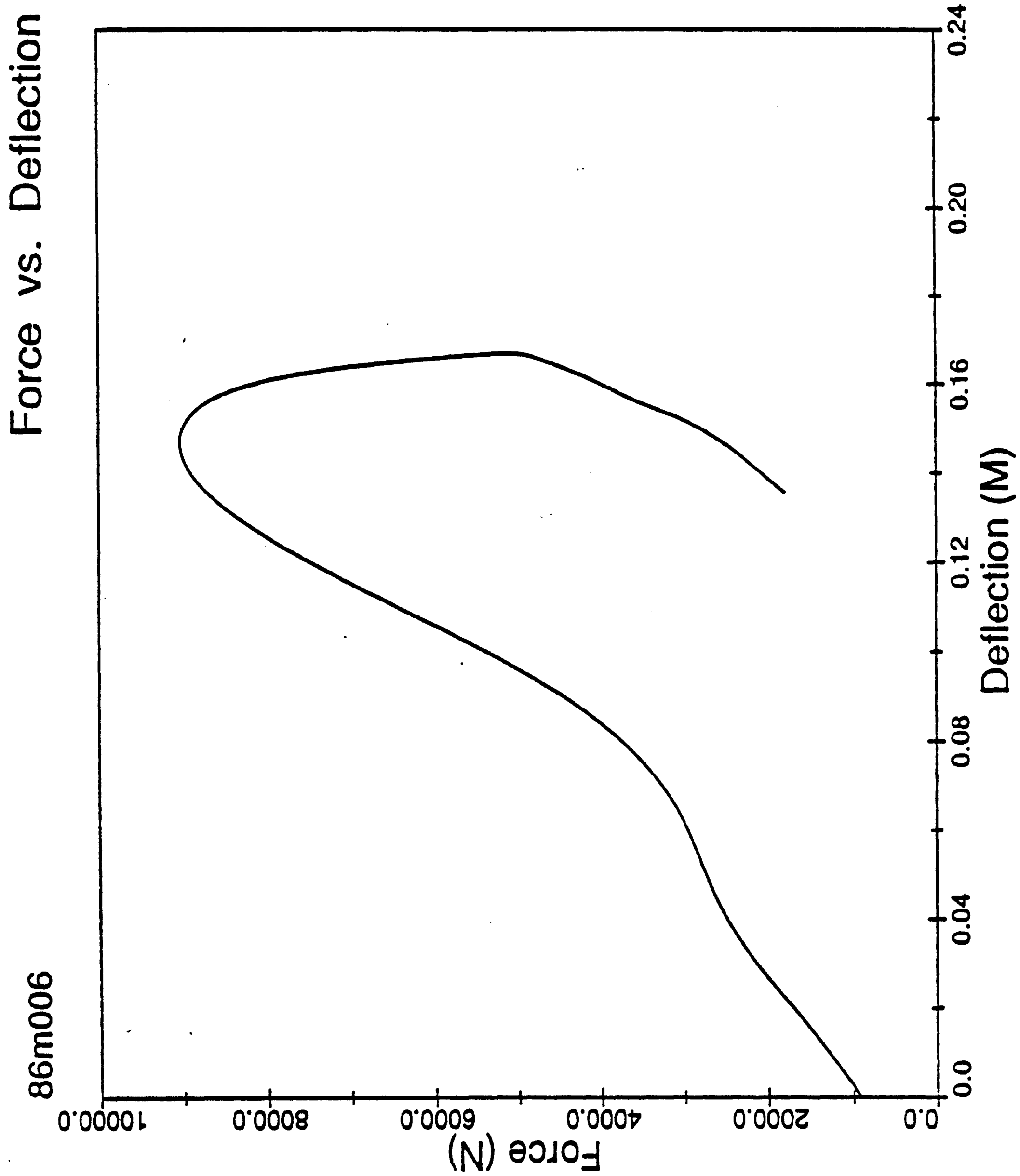
Force vs. Deflection
86m006
Force (N)
0.0
2000.0
4000.0
6000.0
8000.0
10000.0
Deflection (M)
0.0
0.04
0.08
0.12
0.16
0.20
0.24

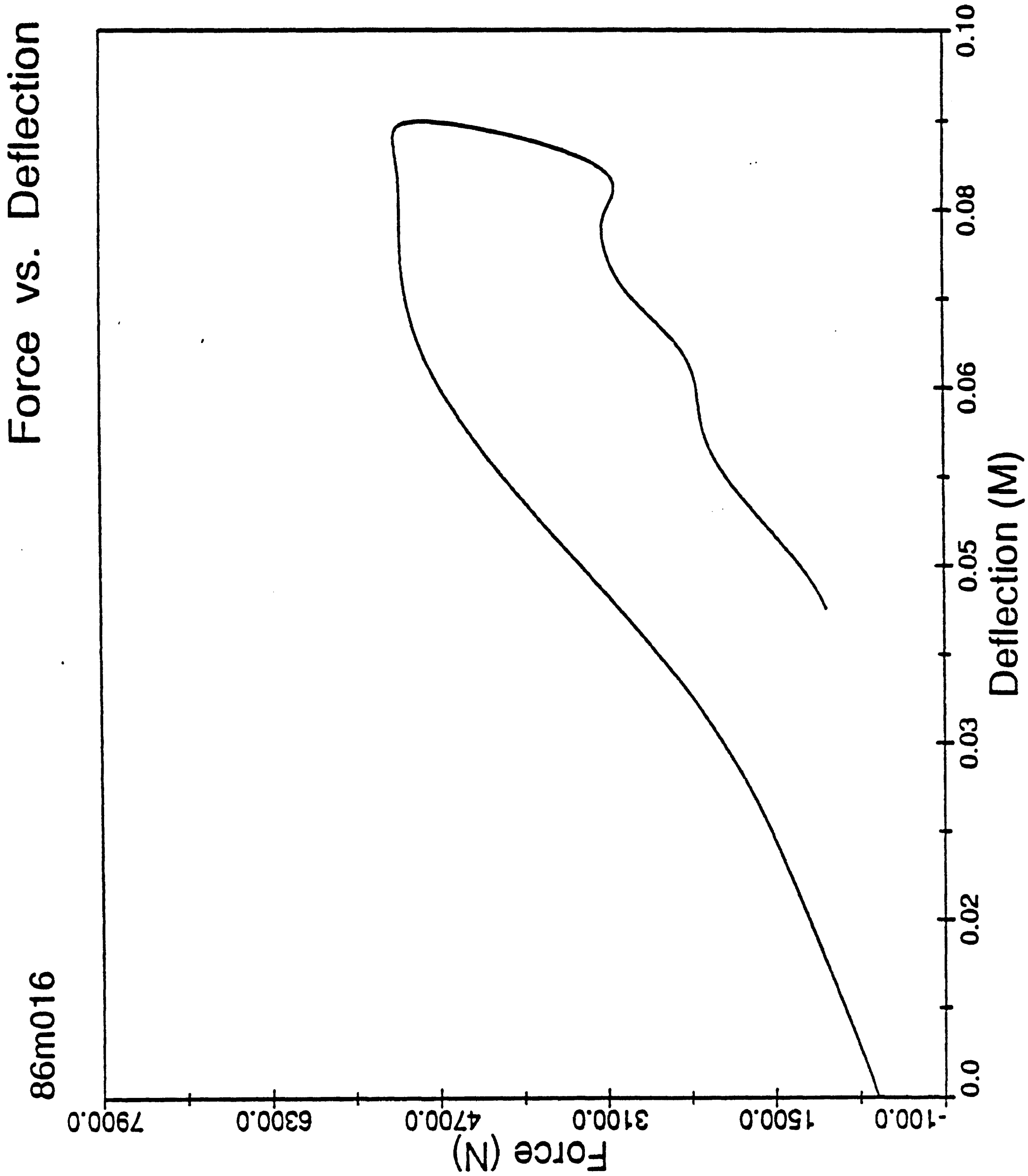

Force vs. Deflection
86m016
Force (N)
7900.0
6300.0
4700.0
3100.0
1500.0
-100.0
Deflection (M)
0.0
0.02
0.03
0.05
0.06
0.08
0.10

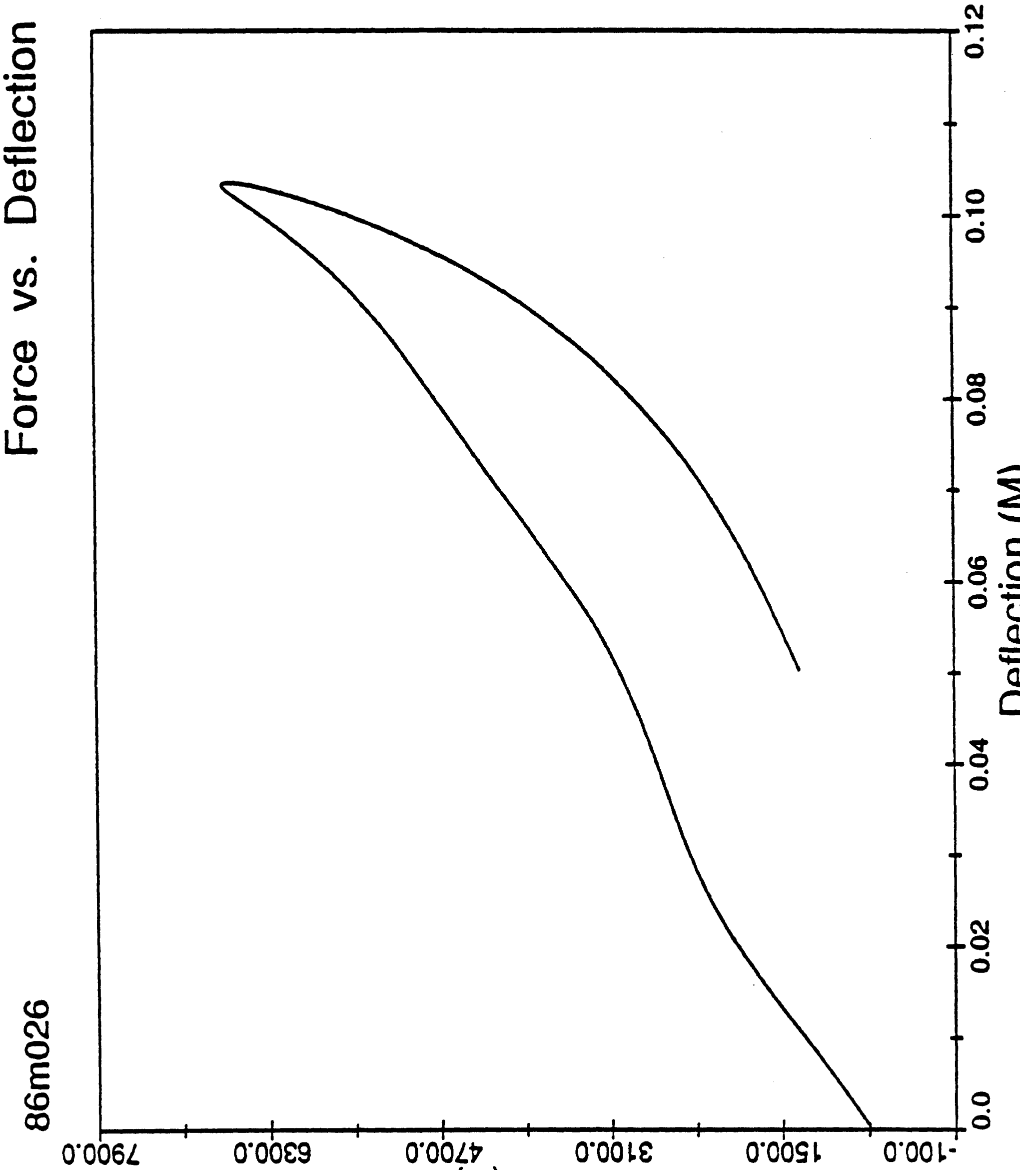
Force vs. Deflection
86m026
Force (N)
-100.0
1500.0
3100.0
4700.0
6300.0
7900.0
Deflection (M)
0.0
0.02
0.04
0.06
0.08
0.10
0.12

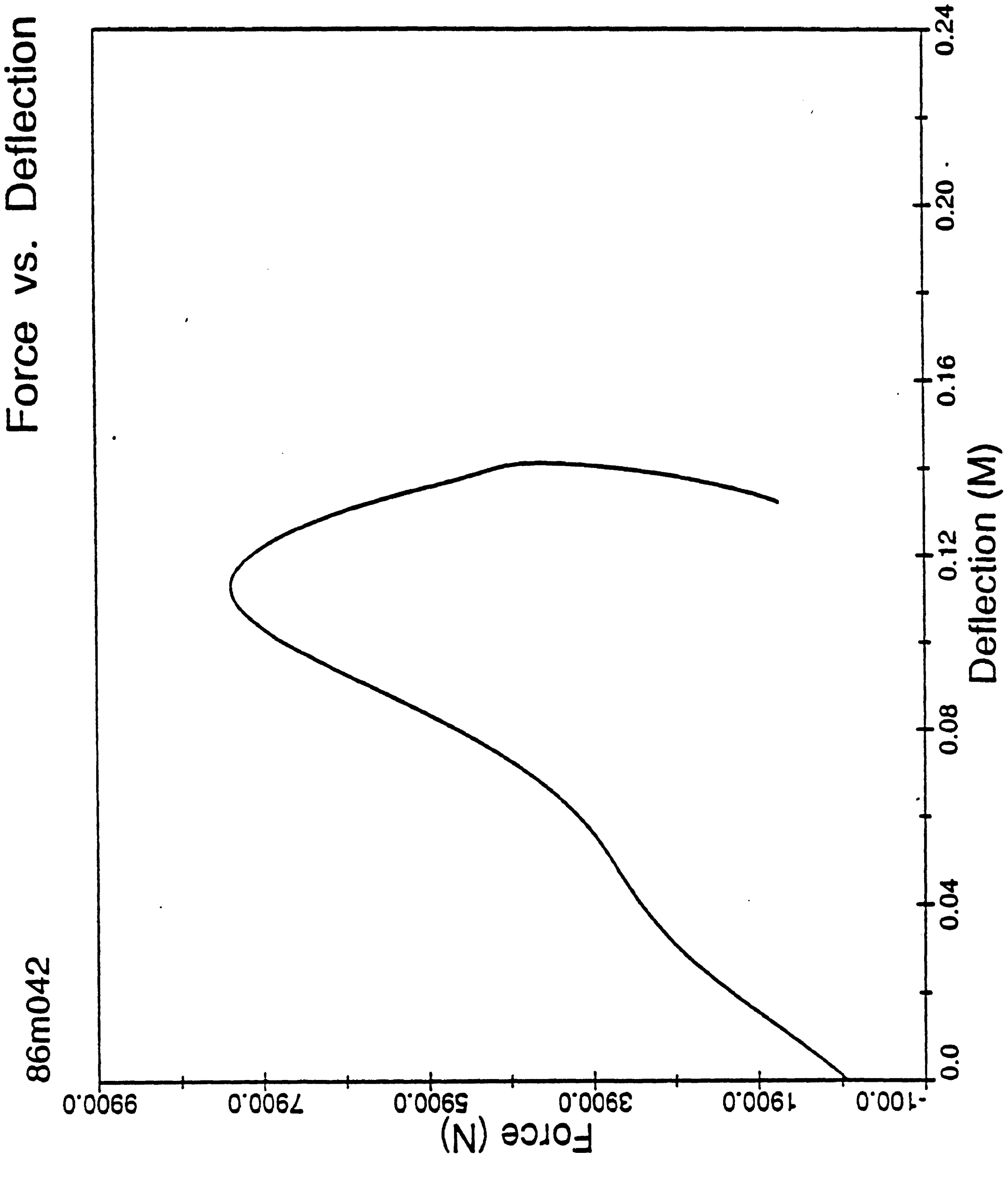

Force vs. Deflection
86m042
Deflection (M)
Force (N)
0.0
0.04
0.08
0.12
0.16
0.20
0.24
-100.0
1900.0
3900.0
5900.0
7900.0
9900.0

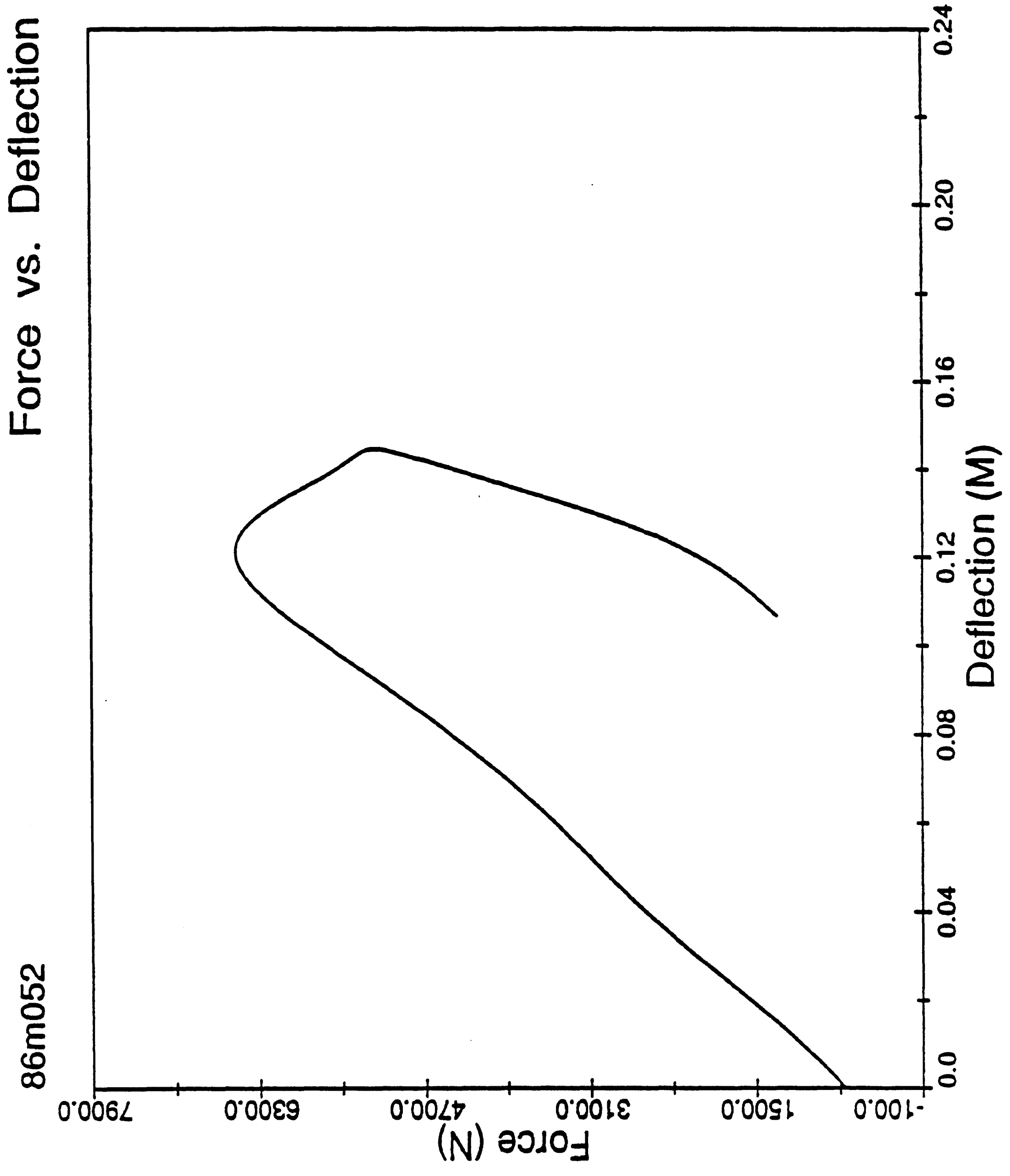

Force vs. Deflection
86m052
Force (N)
-100.0
1500.0
3100.0
4700.0
6300.0
7900.0
Deflection (M)
0.0
0.04
0.08
0.12
0.16
0.20
0.24

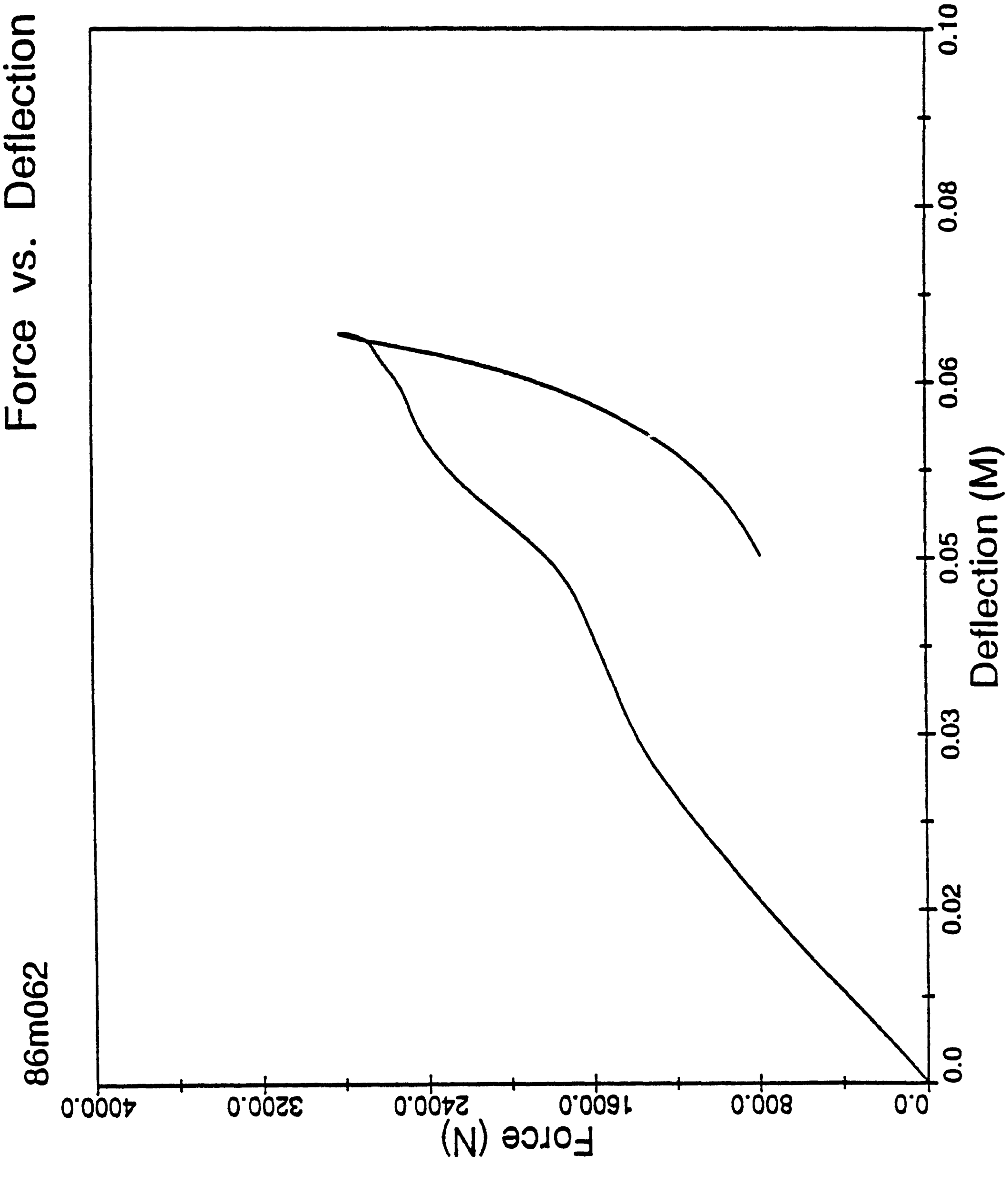
Force vs. Deflection
86m062
Force (N)
0.0
800.0
1600.0
2400.0
3200.0
4000.0
Deflection (M)
0.0
0.02
0.03
0.05
0.06
0.08
0.10

Run ID: *86m006*

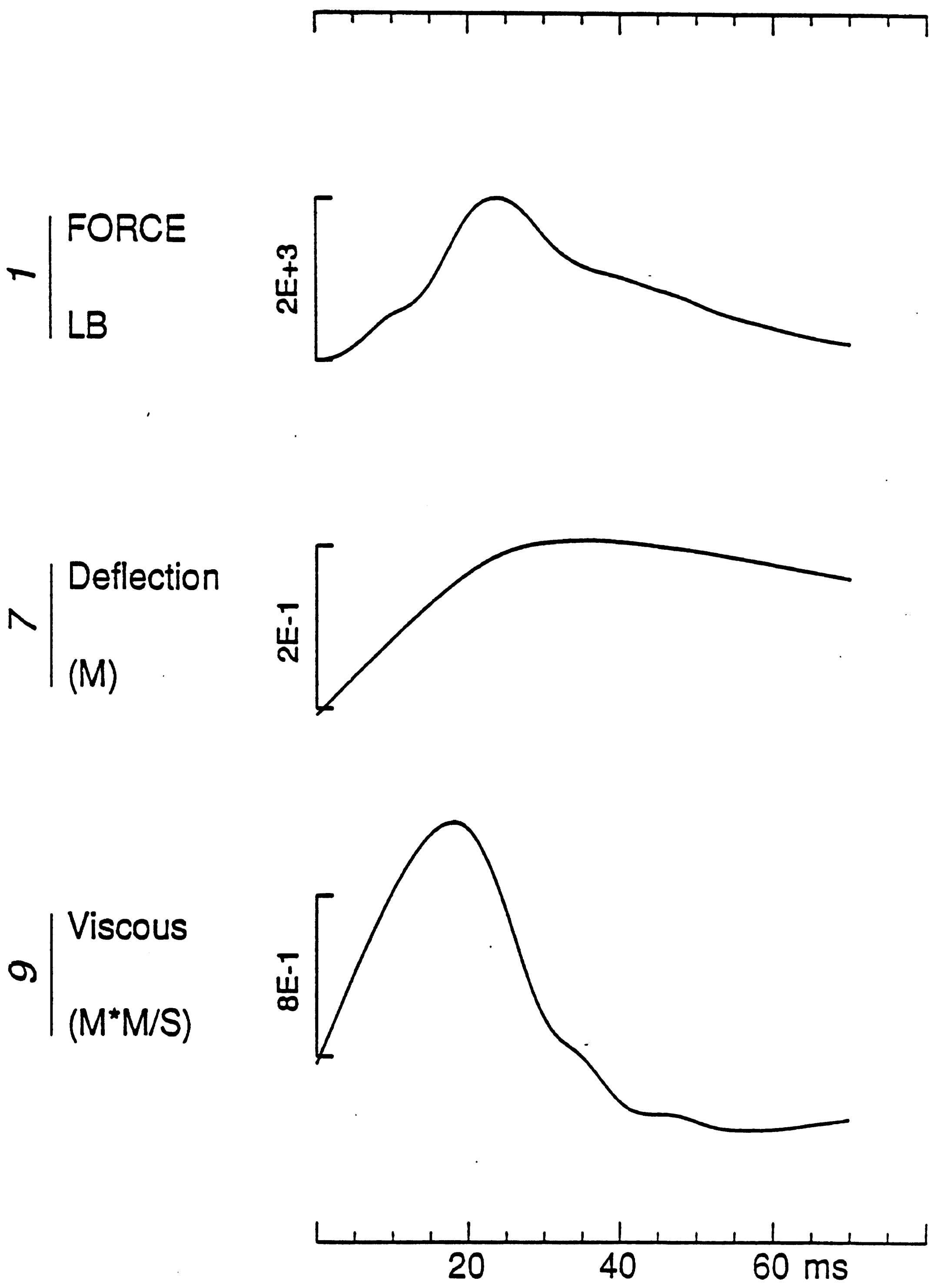

Run ID: *86m016*

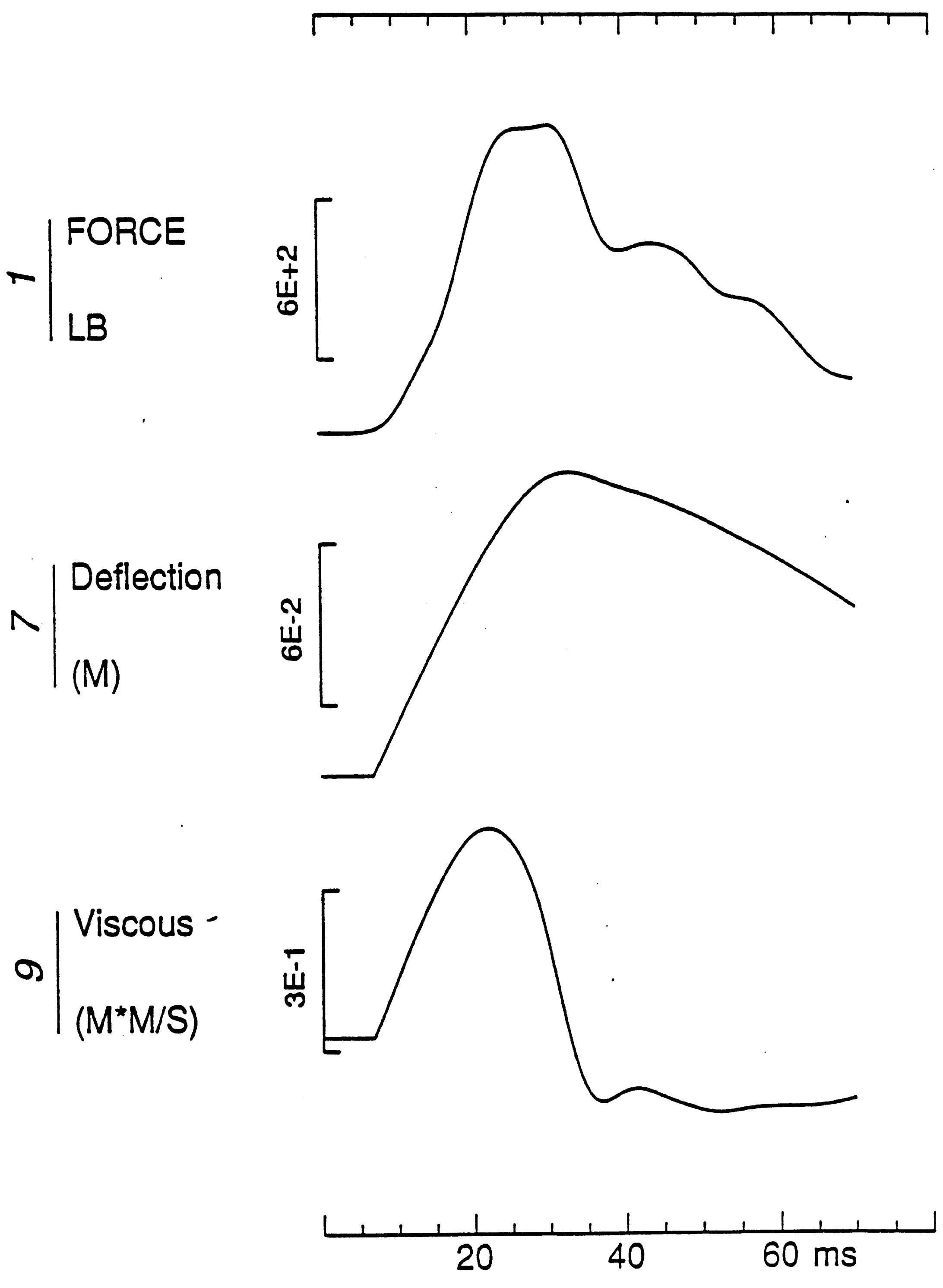

Run ID: *86m026*

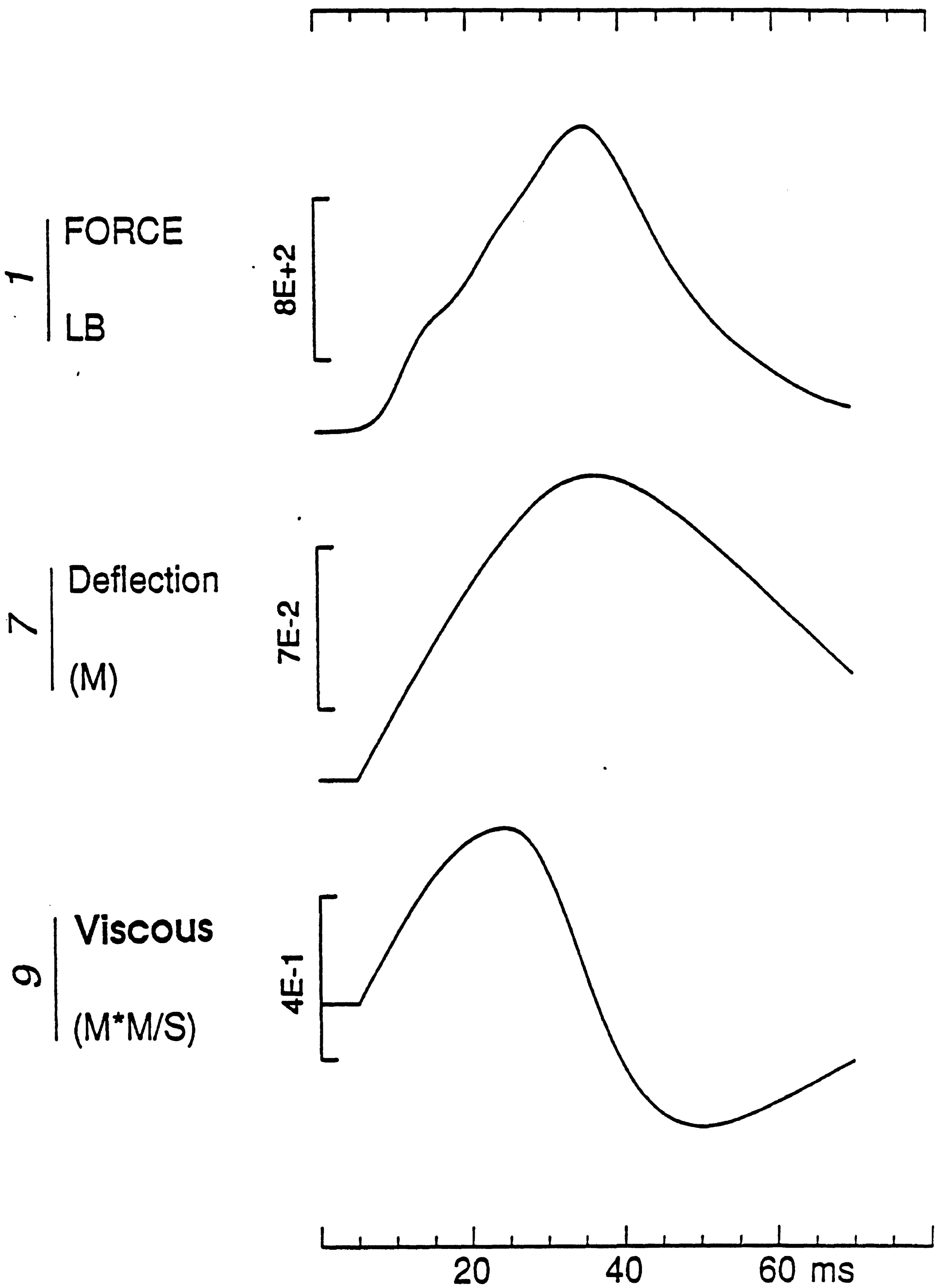

Run ID: *86m042*

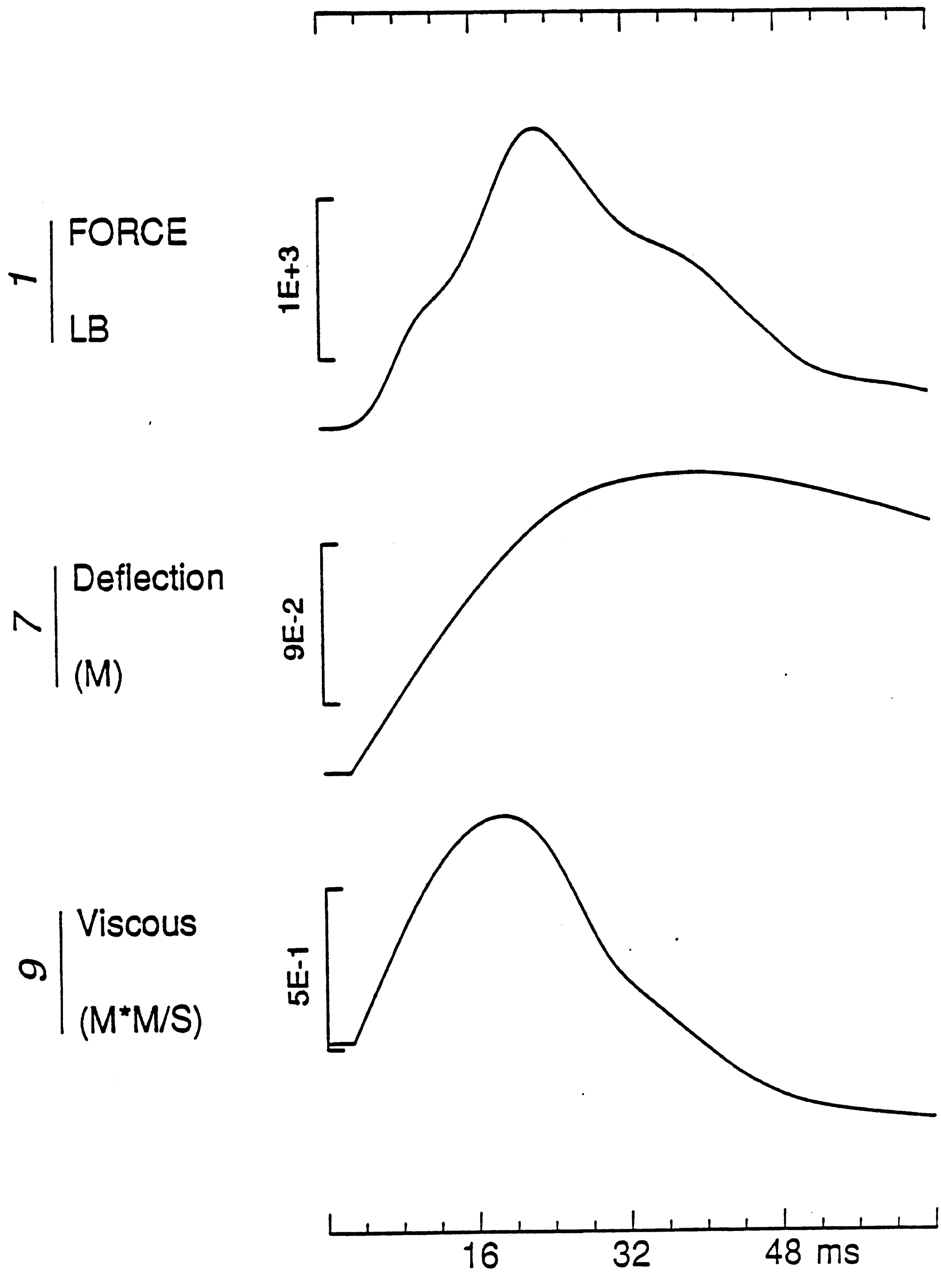

Run ID: *86m052*

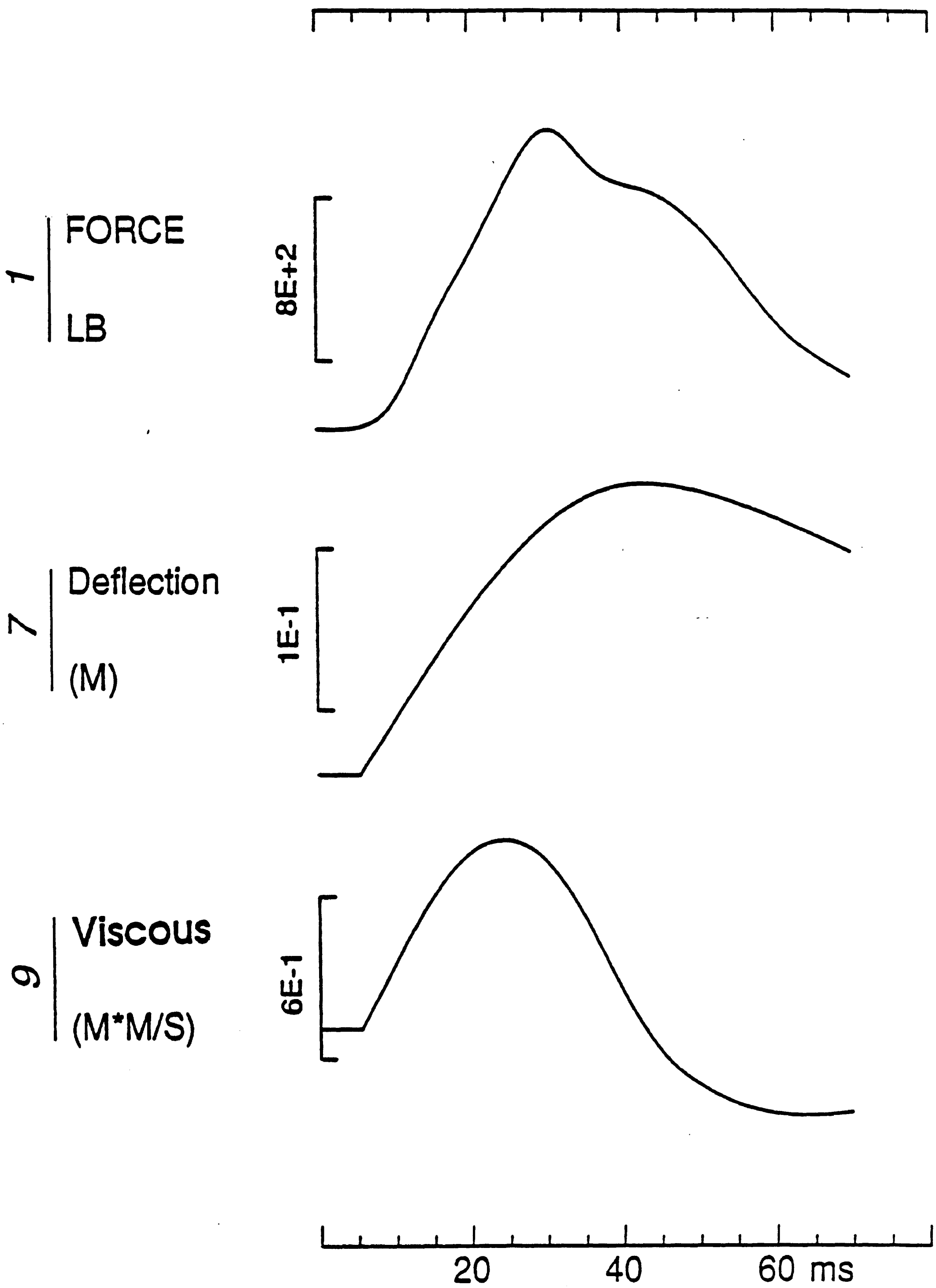

Run ID: *86m062*

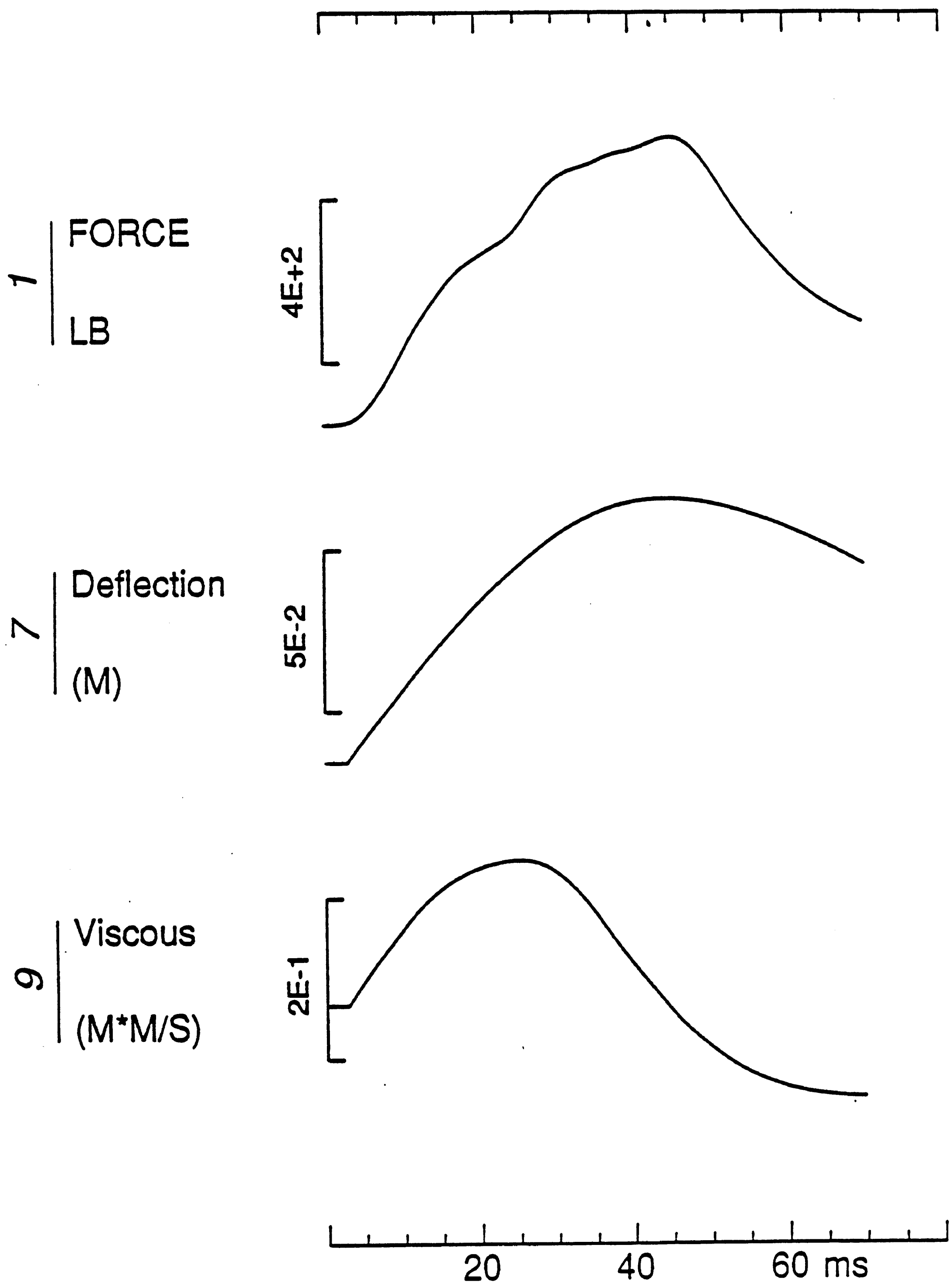

APPENDIX C

Fiscal Year 1988 Test Results

An additional test in this series of steering rim/abdomen impacts was performed in fiscal year 1988. Since the program was subsequently terminated, the results of this test are being reported here.

For this test, M071-18, the impact striking surface was the rigid steering wheel rim used in the previous projects. The steering wheel rim contact point was 2 cm below the bottom of the sternum of the test subject. This test had an impact velocity of 4.6 m/s and produced an AIS 4 liver laceration. This result is consistent with those of the previous tests in that a low-velocity impact by rigid structure to an area directly over the liver produced injury.

One aspect of this test which was different from the previous test series was the use of nine accelerometers for the tracking of the spine during impact. It was hoped that the use of nine accelerometers in place of triaxes would eliminate the need to obtain displacement data from film analysis and, in fact, little difference could be seen between the digitized displacement from film and the displacement obtained from the analyzed nine acceleration output. Although these results are encouraging, and imply that film analysis may not be needed in the future to obtain the injury criteria, this technique requires further validation. The force-deflection plot from this tests and the force-time, deflection-time, and viscous criteria-time curves for this test are shown in the following plots.

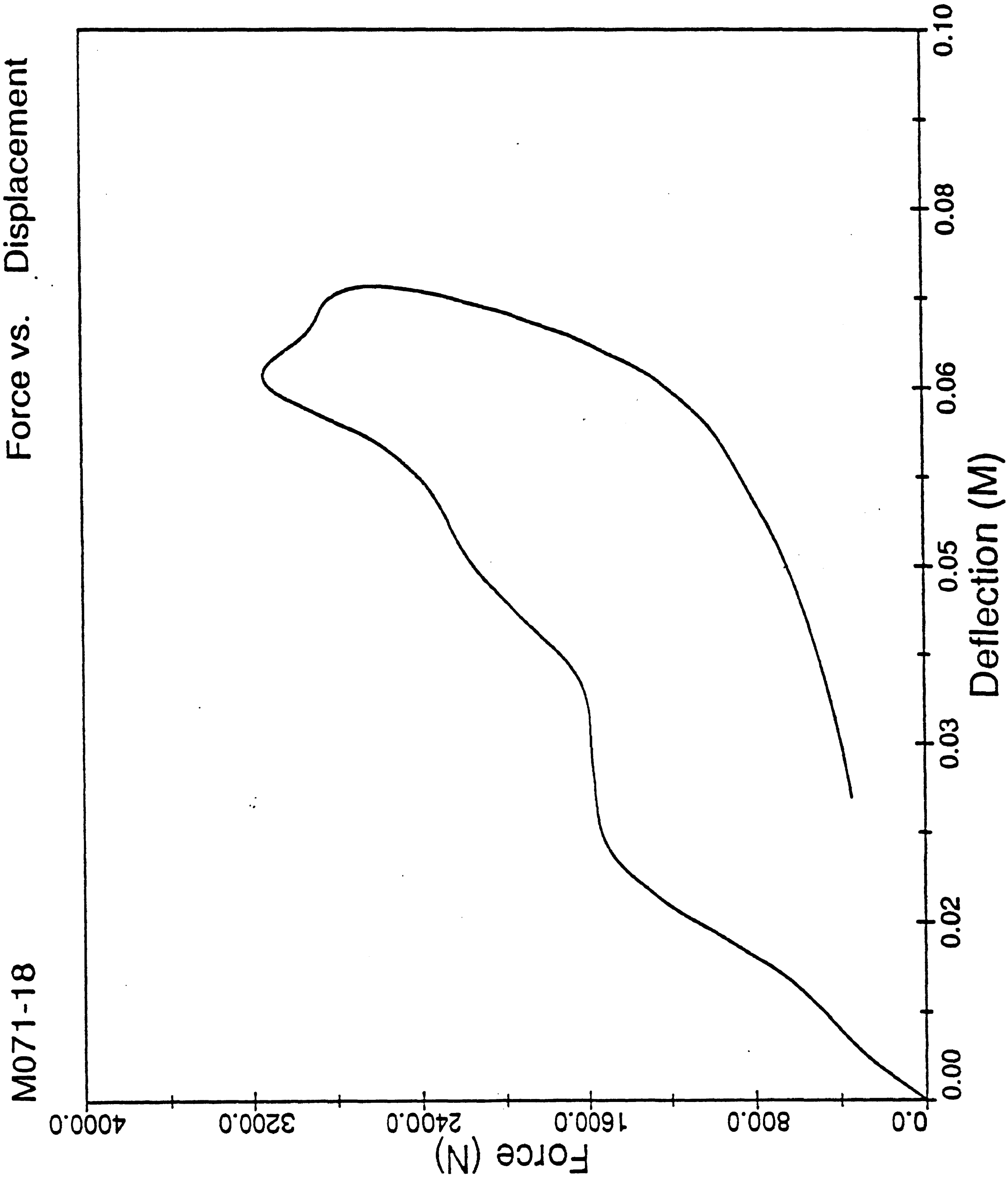
M071-18
Force vs. Displacement
Deflection (M)
0.00
0.02
0.03
0.05
0.06
0.08
0.10
Force (N)
0.0
800.0
1600.0
2400.0
3200.0
4000.0

Run ID: *87M071*